Journal of Archaeological Science 125 (2021) 105273

Contents lists available at ScienceDirect

Journal of Archaeological Science

journal homepage: http://www.elsevier.com/locate/jas

Geochronology of a long Pleistocene sequence at Kilombe volcano, Kenya: from the Oldowan to Middle Stone Age

S. Hoare [a], J.S. Brink [b,c,1], A.I.R. Herries [d,e], D.F. Mark [f,g], L.E. Morgan [f,2], I. Onjala [h], S. M. Rucina [i], I.G. Stanistreet [j,k], H. Stollhofen [l], J.A.J. Gowlett [a,*]

[a] Archaeology, Classics and Egyptology, HLC, University of Liverpool, L69 3BX, UK
[b] Florisbad Quaternary Research, National Museum, P.O Box 266, Bloemfontein, 9300, South Africa
[c] Centre for Environmental Management, University of the Free State, South Africa
[d] The Australian Archaeomagnetism Laboratory, Dept. Archaeology and History, La Trobe University, Melbourne Campus, Bundoora, VIC, 3086, Australia
[e] Palaeo-Research Institute, University of Johannesburg, Auckland Park, Johannesburg, South Africa
[f] Scottish Universities Environmental Research Centre, Isotope Geosciences Unit, Rankine Avenue, East Kilbride, Scotland, G75 0QF, UK
[g] Department of Earth and Environmental Science, University of St Andrews, St Andrews, KY16 9AJ, UK
[h] School of Humanities and Social Sciences, Jaramogi Oginga Odinga University of Science and Technology, P.O. Box 2480-40100, Kisumu, Kenya
[i] National Museums of Kenya, Nairobi, P.O. Box 40658, Kenya
[j] Department of Earth, Ocean and Ecological Sciences, University of Liverpool, L69 3BX, UK
[k] Stone Age Institute, Bloomington, IN, 47433, USA
[l] GeoZentrum Nordbayern, Friedrich-Alexander-University (FAU) Erlangen-Nürnberg, Erlangen, 91054, Germany

ARTICLE INFO

Keywords:
Argon–argon dating
Palaeomagnetism
Oldowan
Acheulean
Paleoenvironments
Middle Stone Age
Rift valley

ABSTRACT

We report a newly extended stratigraphic sequence with associated Palaeolithic sites from the area of the extinct Kilombe volcano in central Kenya. The extended archaeological sequence runs from Oldowan finds, through the Acheulean, and up to the Middle Stone Age. The sedimentary sequences within the Kilombe caldera and south flanks of the mountain have been dated through $^{40}Ar/^{39}Ar$ measurements and palaeomagnetic studies. A series of $^{40}Ar/^{39}Ar$ values date the geological sequence from 2.493 ± 0.095 Ma, near the beginning of the Lower Pleistocene, through to 0.118 ± 0.030 Ma near the Middle to Upper Pleistocene transition. It includes the first entirely new area of Oldowan localities in East Africa south of Ethiopia for thirty years, and the first in a rugged mountainous setting. Trachyte lavas of Kilombe mountain were extruded during and after c. 2.5 Ma, followed by formation of a caldera and subsequent caldera lake, and sedimentation of a sequence of tuffs, diamictites, sandstones, and claystones. Sections in the mid-part of this intra-caldera fill-sequence have produced dates of 1.8–1.7 Ma, associated with an Oldowan industry and fauna dated precisely at 1.814 ± 0.004, and overlain by Acheulean finds at higher level. On the southern outward flanks of Kilombe mountain, a second major sequence is bounded at the base by trachyphonolite and a tuff yielding dates in the range 1.58–1.50 Ma. The main Acheulean archaeological site (GqJh1) falls within the overlying sedimentary sequence and has an age of c. 1.0 Ma, on the basis of a new $^{40}Ar/^{39}Ar$ date for the Three-Banded Tuff and palaeomagnetic reversal stratigraphy. Further $^{40}Ar/^{39}Ar$ dates indicate an age of c. 0.48–0.46 Ma for a marker ashflow tuff (AFT), prominent across the area. At Moricho, west of Kilombe, sediments above the AFT have been dated in the range 270,000–120,000 years and are associated with Middle Stone Age assemblages. In total, these sites attest to hominin activity from an Oldowan horizon dated to 1.8 Ma up to Later Stone Age stone scatters within the last 100,000 years.

1. Introduction

We report new research in and around the extinct Kilombe volcano within the central Rift Valley of Kenya (Fig. 1A and B). The results include the discovery of new traces of hominin activity within the Kilombe caldera, overall description of the stratigraphic sequence, and a

* Corresponding author.
E-mail address: gowlett@liverpool.ac.uk (J.A.J. Gowlett).
[1] Deceased.
[2] Present address: USGS, Denver Federal Center – MS963, Denver Co80225, USA.

https://doi.org/10.1016/j.jas.2020.105273
Received 22 May 2020; Received in revised form 30 September 2020; Accepted 26 October 2020
Available online 19 November 2020

series of $^{40}Ar/^{39}Ar$ dates which show that the sequence spans the entire Pleistocene. The area has previously been best known for its Acheulean archaeology, and its setting of major explosive volcanic centres such as Menengai and Londiani (Bishop 1978; Blegen et al., 2016; Gowlett 1978, 1993; Gowlett et al. 2015, 2017; McCall 1964, 1967; Jennings 1971; Jones 1975, 1985; Jones and Lippard 1979; Riedl et al., 2020). There are two principal volcanic settings in which the sequences were deposited: the fill of the Kilombe caldera, and the southern flanks of the Kilombe volcanic cone (Fig. 2).

1.1. Kilombe volcano and surrounding area

Kilombe mountain is an extinct trachytic volcano, located at the western side of the eastern branch of the East African Rift System (EARS) (Fig. 1A and B), and exposes mainly trachyte lavas and volcaniclastic sediments: its cone is about 20 km across, and it stands to heights of ~2300 m asl. On the south side, the Molo river descends from the Mau escarpment and passes around the southern edge of the mountain. The river eventually flows northwards into Lake Baringo, forming part of the internal drainage system. The northern side of the volcano has few exposures and is not yet explored. The extinct trachytic volcano comprises a caldera about 3 km in diameter, which is now drained by a stream running out through a gorge on the eastern side of the mountain. Erosional downcutting has exposed a series of sedimentary rocks and interleaved tuffs of the intra-caldera fill. A waterfall marks the rapid descent from the central caldera through to the deepest part of the gorge near the caldera edge (Figs. 2, 4 and 5). In the cliff of the waterfall a thick tuff of Middle Pleistocene age is underlain by lacustrine sediments representing the oldest part of the exposed Kilombe caldera fill. Nearby, a trachytic lava is interleaved with this sedimentary sequence and appears to represent the final phase of Kilombe eruptive activity.

The geology of the Kilombe caldera was originally studied and mapped by McCall (1964, 1967), and the wider area subsequently by Jennings (1971) and Jones (1975, 1985, 1988; Jones and Lippard 1979), the latter working within the extensive East African Geological Research Unit (EAGRU) project during the 1970s. Acheulean sites have been known on the southern flank of Kilombe mountain since the 1970s (Bishop 1978; Gowlett 1978) and are the subject of continuing study (Gowlett et al. 2015, 2017; Gowlett 2020).

Our recent research has greatly expanded the range of known geological and archaeological contexts at Kilombe volcano, both within and outside the caldera. In this paper we describe the newly encountered intra-caldera sequence and associated early archaeological (Oldowan and Acheulean) and faunal localities; as well as additional exposures around the southern flanks, especially towards the west at Moricho, where the Middle Stone Age is best characterized and dated.

1.2. New research and an outline succession

Prior to the current research, there was only a low-precision chronological framework for some of the main volcanic events in the area, provided by $^{40}K/^{40}Ar$ ages. These data indicated Lower Pleistocene volcanic activity, and recurrent hominin activity in the Middle Pleistocene (Jones and Lippard 1979). Two palaeomagnetic datum points were obtained for the three-banded tuff on the Kilombe Acheulean Main Site in the 1970s (Dagley et al., 1978; Gowlett 1978, p. 225). They have been checked and added to in recent and ongoing work (Herries et al., 2011).

The age of trachytic lavas of Kilombe mountain temporally constrains the base of the sequence outcropping in the area (Fig. 3). The trachyte units of the caldera rim and cone separate two different

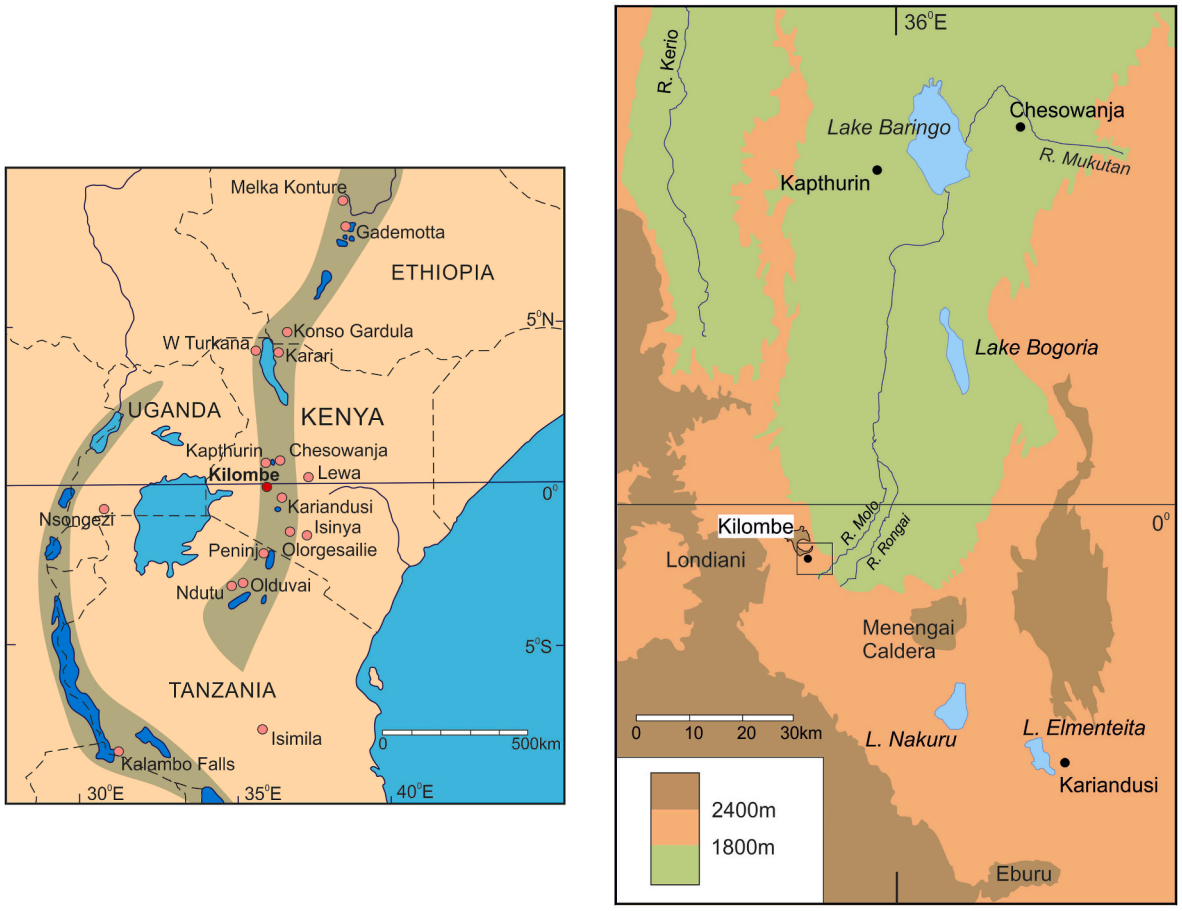

Fig. 1. Location maps of the Kilombe area, (a) in East Africa, (b) in the Kenya Rift Valley.

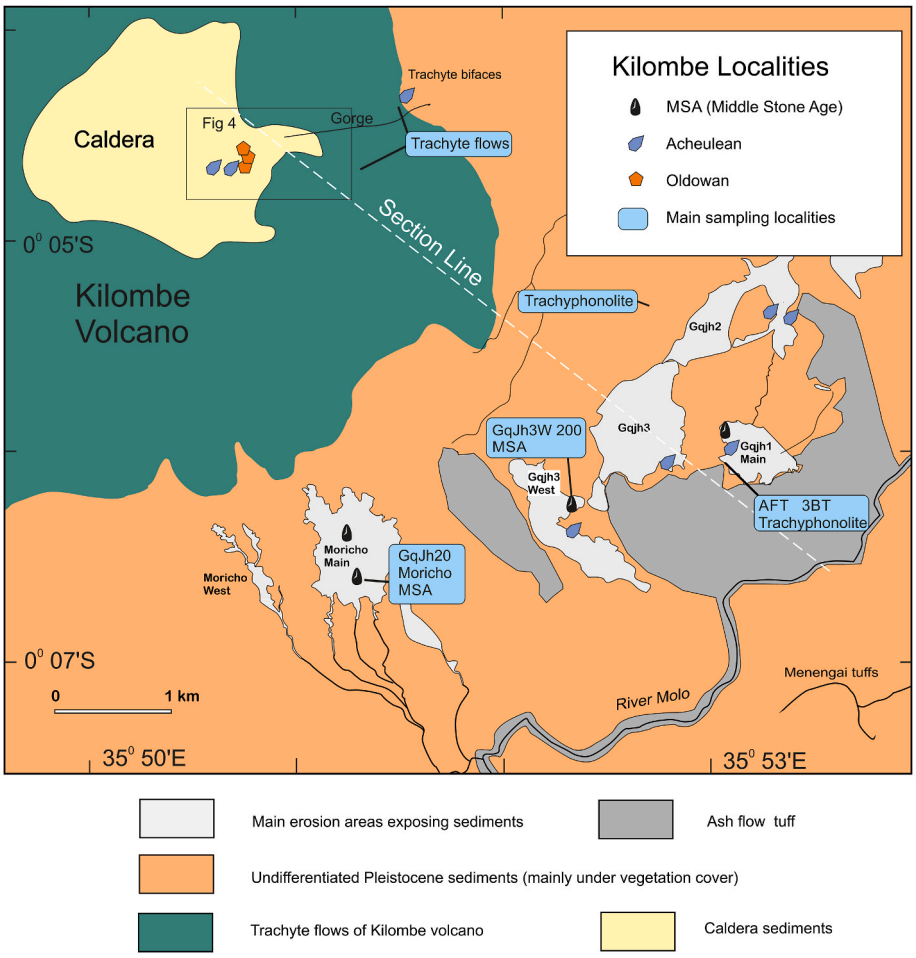

Fig. 2. Map of Kilombe caldera and the southern flanks of Kilombe volcano (based on recent surveys with margins of trachyte following Jennings (1971) and Jones (1975)).

sedimentary sequences. One sequence is contained within the caldera and starts with exposures below the base of the waterfall in the gorge (Fig. 5). This caldera-fill sequence can be traced upwards in two exposures, termed here by analogy 'staircases', which we define here as the *Upper Staircase*, running within the caldera up to a height of ca. 2050 m (Figs. 4 and 5); and the *Lower Staircase*, which runs within the gorge, descending along the edge of a small side gorge and continuing right down to the waterfall and the stream at the base of the gorge (Figs. 4 and 5). Together these exposures preserve a sequence more than 130 m in thickness. The sections exposed in the staircases belong almost entirely to the Lower Pleistocene, as do newly discovered Oldowan and Acheulean archaeological occurrences introduced below; Middle Pleistocene volcanic units however overlie unconformities in the caldera valley and gorge.

The other, largely younger, sequence is exposed on the outer southern slopes of Kilombe volcano (Figs. 2 and 3). Trachyphonolite lava forms a spur that projects southwards towards the Molo River and is topped by an erosion surface. This trachyphonolite lava underlies most of the archaeologically significant sequences outside the volcano, which are exposed mainly in a series of gullies started by minor streams running off the eastern side of the spur, and eventually joining with the Molo River several kilometres downstream. The lava appears to be coeval with and correlate to the series of trachyphonolites that include the Lake Hannington Trachyphonolite (McCall 1964, 1967; Jones 1975, 1985), which is extensive in the rift valley floor to the north of the sites (Griffiths and Gibson 1980). At Kilombe the trachyphonolite is widely overlain by a series of generally reddish sediments, including tuffs. First in the sequence, immediately above the trachyphonolite, come brown and red claystones which were interpreted as weathering products of the lavas (Bishop 1978). The Acheulean Main Site, GqJh 1 (Fig. 2) known since the 1970s lies at the top of these, within a local, broad, shallow clay-filled gully (Bishop 1978; Gowlett 1978; Gowlett et al. 2015, 2017). Above the site level comes the Three-banded tuff (3BT), overlain by a sequence of ca 15 m of reddish tuffs, claystones, sandstones and siltstones (the Farmhouse Cliff sediments), capped by a massive ash flow tuff (the AFT – see below). This tuff marks the beginning of the series of sediments assigned to the "Menengai Assemblage" by Jones (1975), mainly made up of reddish sediments and tuffs up to a thickness of 15–30 m. These were named the Esageri Beds by Jones, and are best exposed at Moricho (Figs. 2 and 3) 3 km west of the Kilombe Main Site (GqJh1), and in large gully systems to the east of the research area (Fig. 2).

In an area within a radius of 3 km from the Acheulean Main Site (GqJh1), and extending along the southern lower flanks of Kilombe Mountain north of the Molo River (Fig. 2), further Acheulean sites have now been located within the Farmhouse Cliff sediments (Gowlett et al., 2015), at higher stratigraphic levels than the GqJh1 site. Middle (MSA) and Later Stone Age (LSA) occurrences have also been found above the AFT within the Esageri Beds, especially at Moricho (Gowlett et al., 2015). They demonstrate that the Kilombe mountain flank sequence offers the potential to elucidate changes in lithic technology over more than a million years, including the transition from the Acheulean to MSA, as also seen to the north in the Kapthurin Formation (Blegen et al., 2018; Johnson and McBrearty 2010; McBrearty 1999; Tryon and McBrearty 2002), and to the south at Olorgesailie (Brooks et al., 2018; Deino et al., 2018).

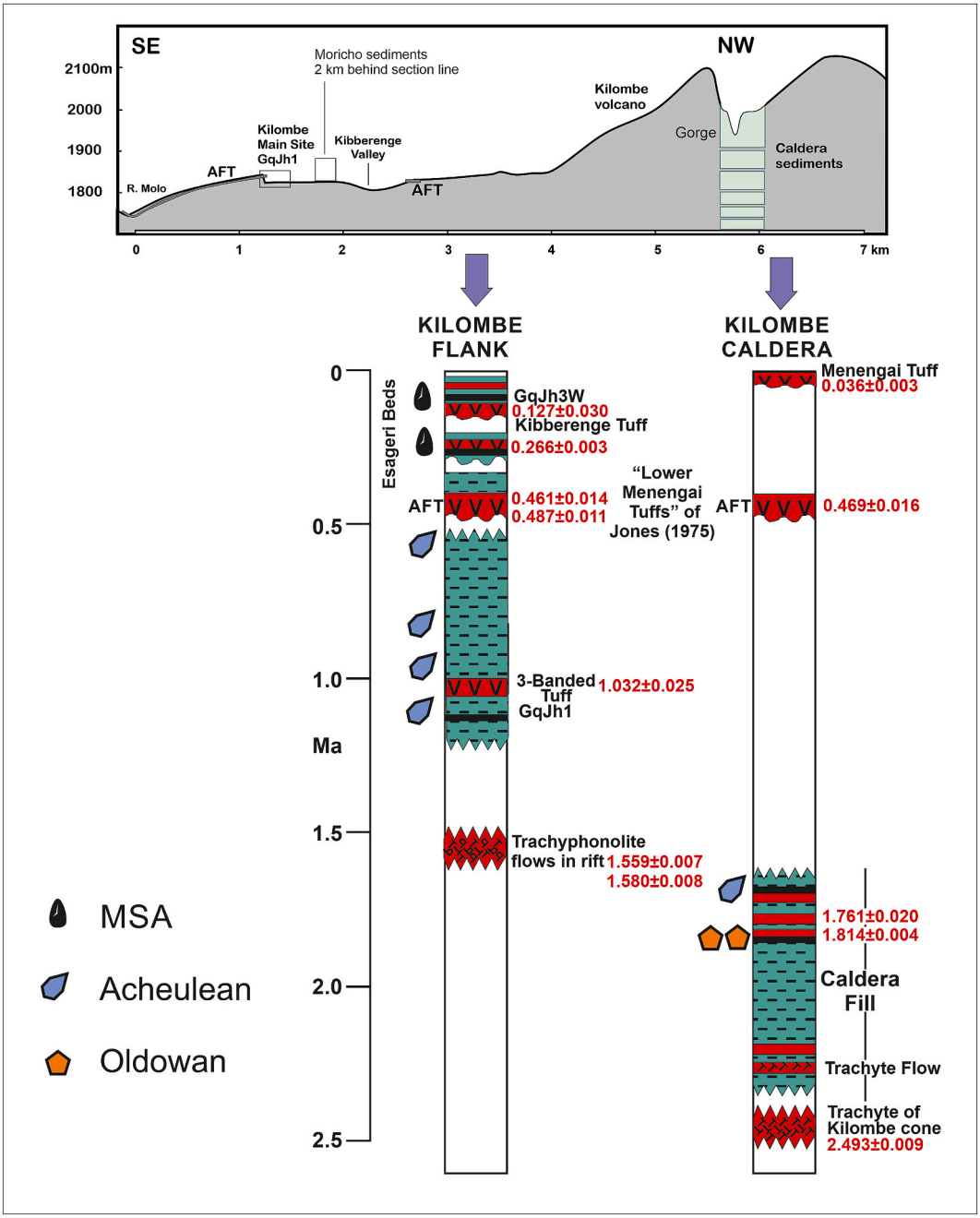

Fig. 3. Stratigraphic overview of the two main exposure series: Kilombe caldera and the mountain southern flank. Above: profile from Kilombe mountain to the Molo River showing sampling areas. Scale in km.

2. Methods

2.1. Survey

Survey has been carried out across the Kilombe mountain flank in continuation from previous studies, using standard map recording methods, aided by GPS and satellite imagery and photography. Sections around the Main Site (GqJh1) and in the caldera have been measured by laser theodolite at <5 cm vertical accuracy. Archaeological sites were given designations using the standard SASES naming system in accordance with National Museums of Kenya registration practice.

2.2. Sample Collection for $^{40}Ar/^{39}Ar$ geochronology

Samples of tuffs and lava flows were collected during field seasons from 2011 to 2017. Samples were taken from primary volcanic deposits as defined by Bishop (1978), except for the intra-caldera volcaniclastics (Kil 2–4 and 2–8) samples, which included both primary tuff and lahar deposits. Fresh material for all the samples was extracted following removal of surface contamination and any weathered material. Each location was recorded using a handheld GPS unit and named according to Bishop's (1978) lithostratigraphy, aside from Kil 2–7.

2.3. Sample preparation and $^{40}Ar/^{39}Ar$ geochronology

A detailed sample preparation routine is discussed by Mark et al.

Fig. 4. Detailed map of Kilombe caldera localities, showing the designated sites (see Fig. 2 for position of this map). Background courtesy Google Earth.

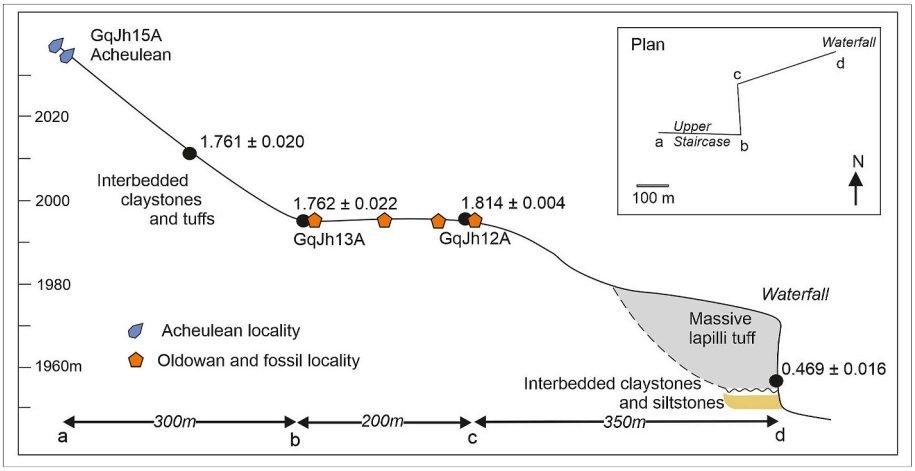

Fig. 5. Outline section of the Kilombe caldera sediments, dating samples and archaeological/faunal localities. Inset map shows position of section line (which does not include the Lower Staircase, cf. Fig. 4).

(2010; 2014), but briefly: feldspars (sanidine) were separated after disaggregating, washing and sieving followed by magnetic and density separations and finally by ultrasonic cleaning in 5% hydrofluoric acid for 5 min. Feldspars were handpicked under binocular microscope for analysis. Samples were irradiated in the CLICIT facility of the Oregon State University TRIGA reactor using the Alder Creek sanidine as a neutron fluence monitor.

$^{40}Ar/^{39}Ar$ analyses were conducted at the NERC Argon Isotope Facility, Scottish Universities Environmental Research Centre (SUERC). Details of irradiation durations, J measurements, discrimination corrections are provided in appendix file DM1. Irradiation correction parameters are shown below.

For J determinations three bracketing standard positions surrounding each unknown were used to monitor the neutron fluence. Eight measurements were made for each bracketing standard position. The weighted average $^{40}Ar^*/^{39}Ar_K$ was calculated for each well, and the arithmetic mean and standard deviation of these three values were used to characterize the neutron fluence for the unknowns. This approach was deemed sufficient as, due to the relatively short irradiation durations, there was no significant variation between the three positions in a single level of the irradiation holder. This also facilitated high-precision measurement of the J-parameter. Note that for all J-measurements no data were rejected.

Samples were analyzed in several batches. Air pipettes were run (on average) after every 5 analyses. Backgrounds subtracted from ion beam measurements were arithmetic averages and standard deviations. Mass discrimination was computed based on a power law relationship (Renne et al., 2009) using the isotopic composition of atmospheric Ar reported (Lee et al., 2006) that has been independently confirmed (Mark et al., 2011). Corrections for radioactive decay of ^{39}Ar and ^{37}Ar were made using the decay constants reported by Stoenner et al. (1965) and Renne and Norman (2001), respectively. Ingrowth of ^{36}Ar from decay of ^{36}Cl

was corrected using the $^{36}Cl/^{38}Cl$ production ratio and methods of Renne et al. (2008) and was determined to be negligible. Argon isotope data corrected for backgrounds, mass discrimination, and radioactive decay and ingrowth are given in the appendix file DM1 (.pdf).

The samples were analyzed by total fusion with a CO_2 laser and measurements made using a MAP 215-50 (MAP2) noble gas mass spectrometer. The mass spectrometer is equipped with a Nier-type ion source and analogue electron multiplier detector. Mass spectrometry utilized peak-hopping by magnetic field switching on a single detector in 10 cycles.

Ages were computed from the blank-, discrimination- and decay-corrected Ar isotope data after correction for interfering isotopes based on the following production ratios, determined from fluorite and Fe-doped $KAlSiO_4$ glass: $(^{36}Ar/^{37}Ar)_{Ca} = (2.650 \pm 0.022) \times 10^{-4}$; $(^{38}Ar/^{37}Ar)_{Ca} = (1.96 \pm 0.08) \times 10^{-5}$; $(^{39}Ar/^{37}Ar)_{Ca} = (6.95 \pm 0.09) \times 10^{-4}$; $(^{40}Ar/^{39}Ar)_{K} = (7.3 \pm 0.9) \times 10^{-4}$; $(^{38}Ar/^{39}Ar)_{K} = (1.215 \pm 0.003) \times 10^{-2}$; $(^{37}Ar/^{39}Ar)_{K} = (2.24 \pm 0.16) \times 10^{-4}$, as determined previously for this reactor in the same irradiation conditions (Renne 2014). Ages and their uncertainties are based on the methods of Renne et al. (2010), the calibration of the decay constant as reported by Renne et al. (2011) and the ACs optimization age (1.1891 ± 0.0009 Ma, 1 sigma) as reported by Niespolo et al. (2017), except where noted. The optimization-modeled age for the ACs standard has accurate quantifiable uncertainties and hence is favoured here over the astronomically tuned ACs age presented by Niespolo et al. (2017). The reason for this is that the astronomical calibration has unknown uncertainty and confidence intervals and uses best guess 'assumptions' to constrain, for example, phase relationships between insolation and climate within the Pleistocene.

3. Results

3.1. $^{40}Ar^*/^{39}Ar$ dates

17 samples were $^{40}Ar^*/^{39}Ar$ dated in total, and the geochronological data and plots are presented in Appendix File DM1. Age computation uses the weighted (by inverse variance) mean of $^{40}Ar^*/^{39}Ar_K$ values for the sample and standard, combined as *R*-values and computed using the method of Renne et al. (2010). Outliers in both single-crystal samples and standards were discriminated using a 3-sigma filter applied iteratively until all samples counted are within 3 standard deviations of the weighted mean ± one standard error. This procedure screened older crystals that are logically interpreted as xenocrysts. Some young crystals were rejected on the basis of low radiogenic ^{40}Ar yields due to analysis of exceptionally small or low-K crystals or as statistical flyer. Processing of the data using the *n*MAD approach of Kuiper et al. (2008) has no impact on the probability distribution plots for each sample. All ages are reported as X ± Y where Y includes all sources of uncertainty as determined through the optimization approach of Renne et al. (2010), using the parameters of Renne et al. (2011), and the standard age of Niespolo et al. (2017). The $^{40}Ar/^{39}Ar$ dates are summarised in Table 1. Further data are provided in supplementary data file DM1. Below we present in more detail the new stratigraphic framework, archaeological occurrences and their relationship with chronological measurements.

3.2. Geochronology and Archaeological relationships

The succession is discussed here in ascending chronological order, (i) in the caldera, and (ii) on the southern flanks of the mountain (Table 1; Figs. 2 and 3). As far as can be determined all dates fit in order within the stratigraphic sequence, within the ranges of reported 1-sigma uncertainty.

3.2.1. The mountain and caldera sequence

The two earliest dates in the series are derived from trachyte flows of the Kilombe volcanic cone. Sample Kil-2–6 was selected from the eastern side of the volcano at the foot of the gorge (Fig. 2), and represents the furthest flow of lava to the east of the mountain, with an age of 2.552 ± 0.038 Ma. Sample Kil-3-1 was collected from the caldera rim (Figs. 2 and 5), immediately to the south of the gorge. The position is high on the mountain and had been interpreted by Jones (1975) as the most recent flow. The age of 2.493 ± 0.009 Ma compares closely with Kil-2-6 and together they are the oldest in the entire series of $^{40}Ar/^{39}Ar$ ages reported here. From the positions of the samples Kil-2-6 and Kil-3-1, it is likely that most of the trachyte flows making up the mountain are somewhat older than ca. 2.4 Ma.

Table 1
Summary of $^{40}Ar/^{39}Ar$ data. Descriptions of each individual age are recorded in supplementary file DM1.

Sample-ID	Age (Ma)	± Ma (1s)	Sampled layer	Polarity	Palaeomag. Constraint
Mountain Flank Sequence					
Kil 2-1	0.111	0.020	Top Seq. Tuff		
Kil 2–7	0.127	0.030	MSA 200		
Kil 3–5	0.266	0.003	Moricho Tuff 105		
Kil 3–4	0.275	0.011	Moricho Tuff 104		
Kil 3-3	0.248	0.004	Moricho Tuff 103		
Kil 1–3	0.461	0.014	AFT	N	<0.78 Ma (Brunhes Chron)
Kil 1–4	0.487	0.011	AFT	N	<0.78 Ma (Brunhes Chron)
Kil 2-2	1.032	0.025	3BT	R	>0.78 Ma (Matuyama Chron)
Kil 2–5	1.509	0.034	Tuff with grass prints		
Kil 1–2	1.559	0.007	Trachyphonolite		
Kil 1-1	1.580	0.008	Trachyphonolite		
Caldera Sequence					
Kil 1–5	0.469	0.016	Tuff at Waterfall	N	<0.78 Ma (Brunhes Chron)
Kil 2–4	1.761	0.020	Tuff in Upper Staircase		
Kil 2–8	1.762	0.022	Tuff in GqJh13A		
Kil 3-2	1.814	0.004	Tuff in GqJh12A		
Trachytes of Kilombe volcanic cone					
Kil 2–6	2.552	0.038	Trachyte flow base of gorge		
Kil 3-1	2.493	0.009	Trachyte flow Caldera rim		

All ages calculated using the decay constants of Renne et al., 2011.
Ages referenced against the Alder Creek sanidine age of Niespolo et al., 2017 (optimization, 1.1891 Ma).
Age calculations used the atmospheric $^{40}Ar/^{36}Ar$ of 298.56 ± 0.31 (Lee et al., 2006; Mark et al., 2010).
All ages include systematic uncertainty as calculated using the optimization model of Renne et al., 2010.
Polarity: N = normal and R = reversed.

Fig. 6. The Upper Staircase of tuffs and sediments visible in Kilombe Caldera. Arrows indicate the positions of sites GqJh13A, Oldowan, and GqJh15A, Acheulean.

The $^{40}Ar/^{39}Ar$ ages of ca. 2.4–2.5 Ma are older than the single earlier age determination reported by Jones and Lippard (1979): their sample (14/1) gave a $^{40}K/^{40}Ar$ age of 1.90 ± 0.15 Ma. Coordinates which they provided for that sample are 35.50E/00.03S, indicating a point on the northern side of Kilombe volcano, about 3–4 km NW of our sampling points (Fig. 2, sample 14/1). There are two potential scenarios to explain the age difference: (1) incomplete extraction of radiogenic ^{40}Ar during laboratory heating may have caused an artificially young age constraint, or (2) that the sample may be from a unit younger than the trachytes sampled in our research. In total, Jones (1975) recognised more than 13 individual volcanic events. The larger Londiani volcano, a few km to the west of Kilombe (Fig. 1B), is a similar trachyte volcano (Jennings 1971), and provided a $^{40}K/^{40}Ar$ age of 3.1 ± 0.1 Ma (Jones and Lippard 1979). These results are consistent with the interpretation first set forward by Jennings and Jones that Londiani Volcano was active in the late Pliocene, and Kilombe was a centre of volcanic activity during the earliest Pleistocene.

3.2.1.1. Kilombe caldera sequence. The caldera-fill sequence rises to a height of ca 2 km, just below the summit of the collar of the volcano, and most probably extends over the entire caldera diameter of ca. 3 km (McCall 1967; Jennings 1971) (Figs. 2 and 4). The sediments covering approximately 10 km^2 are largely covered by vegetation but are accessible close to the surface and are exposed in a number of outcrop areas. The caldera fill comprises a series of horizontally bedded tuffs (see also Ridolfi et al., 2006) and massive volcaniclastic breccia and sandstones, interbedded with claystones, thin sandstones and siltstones. This sequence is currently best exposed in a trackway ascending from a dammed pool in the caldera centre, and comprises the *Upper Staircase* sequence (Figs. 5 and 6). Deeper portions of the caldera-fill are exposed in a *Lower Staircase* (Fig. 4) descending into the gorge, and lead down to and below the waterfall section. Running from East to West, the entire set of exposures in the *Upper Staircase* rises 100 m along a length of ca. 500 m. The *Lower Staircase* runs approximately SSW to NNE along 250 m, descending from ~1980 to ~1920 m (Fig. 4).

The first fossil bones from the sequence were found by the farmer Mr Philip Kogai during the digging of a latrine pit at a level near the base of the Upper Staircase section (This is confirmed to be the same level explored in site GqJh 13A, which is a few m south of the latrine: Fig. 5). In a striking case of research impact, stimulated by knowledge of investigations in the area outside the volcano he reported the bones to the Museums, and they were confirmed as representing mineralised fossil material contained within a volcano-sedimentary unit.

The well-preserved fossils found subsequently at these levels in the Upper Staircase sequence, include extinct bovids and hippopotamus identified by JB as *Hippopotamus gorgops*. Since 2012, road improvements to the trackway have obscured details of the stratigraphy, but it has been possible to clean new sections in the side of the road, and to identify within the staircase many successive tuffs, volcaniclastic sandstones and diamictites resulting from lahars (volcanically related mudflows), separated by claystone units, which include siltstone and sandstone interlayers. The many tuffs indicate recurrent eruption of probably more than one nearby (proximal) to distal volcanic sources, and the lahars indicate mudflows reworking material within the confines of Kilombe caldera itself. Individually, units are 20 cm up to 100 cm thick, and separated by units of claystone, which exhibit a "waxy" texture (cf Hay 1976:42), related to smectite content, indicative of deposition in a saline-alkaline lake.

Three of our $^{40}Ar/^{39}Ar$ dated samples relate to the lower part of the Upper Staircase, and to finds made subsequently at the same levels in fields north of the road which exposes the staircase stratigraphy. The most precise date comes from a locality (GqJh12A) investigated with the help of the farmer, Mr Kogai, 200 m to the north of the Upper Staircase (Fig. 4). A tuff sample Kil 3-2 taken here yields a $^{40}Ar/^{39}Ar$ age of 1.814 ± 0.004 Ma. Hippopotamus and bovids are represented at this locality, embedded within the tuffaceous sequence. Sample Kil-2-8, from the same horizon in the Upper Staircase, yielded a less precise but compatible date of 1.762 ± 0.022 Ma; this came from a thin tuff immediately underlying the bone and artefact finds (locality GqJh13A) (Figs. 3–5). . A third date of 1.761 ± 0.020 Ma (Kil-2-4) from 15 m higher in the Upper Staircase constrains the minimum age of archaeological and faunal finds in this area, the three dates being consistent with the identification of *H. gorgops* in the assemblage. About 30 m of sedimentary sequence then overlies the upper dated horizon, culminating in a fairly horizontal surface running across the central part of the caldera.

The two $^{40}Ar/^{39}Ar$ ages for Kil 2–4 and Kil 2–8 are in stratigraphic order, but considering their uncertainties they are statistically indistinguishable. With the third $^{40}Ar/^{39}Ar$ age (Kil-3-2) they demonstrate an Early Pleistocene age for the fossil localities, approximately contemporary with the part of the sequence at Olduvai including the Bed I/Bed II boundary (Hay 1976; Blumenschine et al., 2003; Deino 2012; Stanistreet et al., 2018). The precise age for Kil 3-2 specifies the bone assemblage

Table 2
Main archaeological and faunal localities of Kilombe mountain (surf. = surface finds, exc. = excavated).

SASES Locality	Area	Character	Artefacts
GqJh1 MSA	S Flank, Kilombe Main Site	MSA	14 exc.
GqJh3W-200	S. Flank, Kilombe West	MSA	17 exc., ~100 surf.
GqJh20	S. Flank, Moricho, central	MSA	5 exc., 20 surf.
GqJh3 KW	S. Flank, Kilombe West	Acheulean	14 surf. bifaces
GqJh2	S. Flank, Kilombe SE Gullies	Acheulean	15 exc. 30 bifaces
GqJh1	S. Flank, Kilombe Main Site	Acheulean	2000+ exc. 500+ surf. (bifaces)
GqJh15A	Caldera, Upper Staircase	Acheulean	75 exc., 7 surf.
GqJh13A	Caldera, Upper Staircase	Oldowan	~100 exc. + fauna
GqJh12A	Caldera, N of Upper Staircase	Oldowan	1 exc. + fauna
GqJh12B	Caldera, N of Upper Staircase	Oldowan	3 surf. + fauna
GqJh12C	Caldera, N of Upper Staircase	Oldowan	~15 exc. + fauna

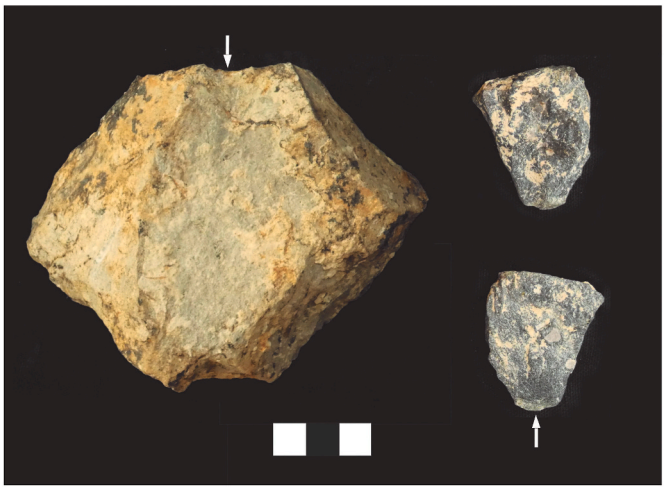

Fig. 7. Oldowan artefacts of trachyte, site GqJh13A. Left: simple core, showing detachment area of a single main flake. Right: flake, dorsal and ventral views. Scale 3 cm.

here as equivalent to slightly older than Tuff IF at Olduvai in topmost Bed I.

Stone artefacts have been found from four localities at these levels, all of which also contain fauna (Table 2). They are Oldowan-like in general character, consisting of cores, core-tools and flakes, and are mainly made of trachyte. Their significance is discussed further below. At locality GqJh13A, at the base of the Upper Staircase, there is proof of multiple bones *in situ*, associated with around 100 excavated stone finds (Fig. 7); smaller numbers of finds come from localities GqJh12 A, B and C (Fig. 4, Table 2). A large core was also found at an isolated exposure on the south side of the gorge, at an elevation of ~1985 m.

The Upper Staircase ascends approximately 40 m along a length of 200 m, and is mainly composed of a series of interbedded mudflows, tuffs and claystones. Towards the top is a series of mudflow units. These contain artefacts of undoubted Acheulean character, including several bifaces and biface flakes. Artefacts are found scattered within the mudflows and are also found concentrated at one interface in a clayey lens. All the main elements of early Acheulean assemblages are represented, including ~6 bifaces (Fig. 8), several cores and probable heavy-duty scrapers, and a number of flakes. Some flakes indicate simple working of a core, but one is interpreted as a handaxe trimming flake. The significance of these finds is discussed further below. Further Acheulean finds in the caldera were made in 2019 and the complete assemblages will be reported on separately.

3.2.1.2. The Lower Staircase and gorge development. Tuffs and other sediments can also be traced at lower levels in the gorge leading out of the caldera. They can be followed in the *Lower Staircase* (Figs. 4 and 5) which descends along the western face of a small side gorge on the south side of the main gorge, and then along the spur between the side gorge and main gorge down to the level of the stream. Exposures can also be traced westward intermittently along the south side of the main gorge to the point where it terminates with a vertical rock face, over which the stream descends around 25 m in the waterfall. At the waterfall a far younger very thick tuff fills and covers a deeply incised unconformity surface that cuts down into horizontal thinly laminated lacustrine deposits, in places displaying ripple marks. These and underlying lacustrine sediments appear to represent stratigraphically the oldest exposed levels of the caldera-fill sequence. A trachyte lava unit at a slightly higher level extruded within a succession of diamictites deposited by mudflows, and is interbedded with that oldest sequence, probably recording the last event in the history of the activity of Kilombe volcano itself. Further dating and palaeomagnetic studies may give added chronological resolution to events between the early lavas of the volcanic cone at ca 2.5 Ma and the dated tuffs of the caldera-fill at ca 1.8 Ma.

Within the caldera area modern streams cut down through the caldera-fill, joining to make the modern gorge. However there have been earlier phases of gorge development. At the waterfall a proto-gorge incises deeply through the older caldera-fill sequence and this incision is filled by a thick coarse lapilli ash tuff Kil 1–5 which has been $^{40}Ar/^{39}Ar$ dated at its base to 0.469 ± 0.016 Ma (Fig. 5).

This Middle Pleistocene age shows that the tuff is far younger than all the tuffs and interleaved lacustrine units just described. We deduce that the pronounced unconformity, on which the tuff sits, cuts down deeply through the older sequence. The lacustrine sequence underlying the massive tuff exhibits reversed magnetisation (thus an age >780 ka based on the date of the Brunhes Matuyama transition: Mark et al., 2017), whereas the sequence above and including the tuff exhibits normal polarity, emphasizing the magnitude of the erosional break at the base of the tuff. Jones (1975; also Bishop 1978) identified an Ash Flow Tuff (AFT) in the region which he placed as the basal unit of his Menengai Series, since he linked the sediments with the earliest eruptions of

Fig. 8. Left, Acheulean handaxe of trachyte from Kilombe caldera site GqJh15A; centre, handaxe from site GqJh2 on the southern flank of the mountain; right, a handaxe found less than 1 m below the AFT in the same GqJh2 area, and hence the youngest biface yet known from Kilombe. Scale in cm.

Menengai (or a proto-Menengai in his terms). Menengai volcano lies about 20 km south of Kilombe, and the tuffs are more thickly developed approaching it from the north side (Jones 1975). The Ash Flow Tuff occurs extensively on the southern flanks of Kilombe, and was also mapped by Jones as occurring in the calderas of Londiani and Kilombe: in 2018 it was observed on the north side of the stream channel within Kilombe Caldera. The date of the incision-fill tuff in the gorge is statistically indistinguishable from those for the Ash Flow Tuff (see below), and we correlate them provisionally.

In places lower down the stream course within the gorge remnants of tuffs and mudflows are visible. From this evidence it seems likely that a stream was already draining the caldera and cutting through caldera-fill sediments that were deposited during the Matuyama Chron prior to ca. 470 ka.

In summary, the current research has established the presence of extensive early Pleistocene sediments within Kilombe caldera, and temporally constrained them to between ca. 2.4 and 1.7 Ma, with extensions to that time range possible. Previously the entire caldera-fill was mapped by Jennings (1971) and Jones (1975) as far younger sedimentation. It is now possible to state with certainty that two different units are involved, separated by a considerable time interval. The bedded tuffs are far older than the massive tuff, which has an age indistinguishable from that of the AFT outside the caldera (see below dates Kil 1–3 and 1–4). The late Pleistocene Menengai Tuff (Jones 1975; Blegen et al., 2016; Blegen 2017) is also present within the caldera to the south of the main drainage way, also sitting on an unconformable incision surface.

3.2.2. *The succession on the southern mountain flanks*

3.2.2.1. Basal trachyphonolite. On the southern side of Kilombe Volcano, Pleistocene sediments cover an area of at least 6 × 3 km, mantling its lower slopes (Fig. 2). At the base is a greenish-grey, feldspar-phyric, trachyphonolite lava (Bishop 1978), in places flow-laminated, which forms a spur extending from the south side of the mountain. Although it is largely covered by younger sediments, the trachyphonolite is widespread and exposed in many places, and usually has an irregular undulating top surface. A direct stratigraphic relationship with the trachytes of Kilombe mountain has not been observed (Bishop 1978; Jones 1975), but it is certainly less altered. It has yielded two dates at localities about 1 km apart, the first close to the archaeological Main Site (GqJh1), and the second at the Kapsigat road junction nearer to Kilombe mountain (Fig. 2). Dates yielded are 1.580 ± 0.008 Ma (Kil-1-1) and 1.559 ± 0.007 Ma (Kil-1-2) respectively. The two $^{40}Ar/^{39}Ar$ dates overlap within 2 standard deviations. A previous $^{40}K/^{40}Ar$ age on the trachyphonolite published by Jones and Lippard (1979) had given the age of 1.70 ± 0.05 Ma (their sample 14/369). Its coordinates 35.52E/00.09S (Jones and Lippard 1979) put the sampling point close to the Molo River about 2 km NE of Rongai, and some kilometres SW of our research area.

As noted above, no contact has been detected between the trachyphonolite and the trachytes of Kilombe mountain (Bishop 1978; Jones and Lippard 1979), and the stratigraphic relationship has been unclear. Jones (1975) correlated them to the Lake Hannington Trachyphonolite. The new $^{40}Ar/^{39}Ar$ dates show that the trachyphonolite substantially postdates the trachytes of Kilombe volcano itself, and substantially altered the landscape.

The new trachyphonolite ages provide the earliest timings for the archaeological and environmental sequence on the southern flanks of Kilombe mountain. It is worth noting that they are also similar to ages for lavas at the base of the Kapthurin Formation 70 km to the north, which are dated at ~1.57 Ma. (Deino and McBrearty 2002; McBrearty 1999 Tryon and McBrearty, 2002), and represent part of the same general set of volcanic lava outputs within the Rift.

The trachyphonolite lavas outcrop at the present surface in substantial outcrops, but are usually overlain by several metres of red and brown claystones, occasionally containing faunal remains (Bishop 1978; Brink in Gowlett et al., 2015), and which have been previously interpreted to represent accumulated weathering products from the basal lavas (Bishop 1978). Bishop noted a yellowish fine bedded tuff with grass prints occurring within the brown clays on the Acheulean Main Site (GqJh1). This is about 1.5 m below the main artefact horizon and has now been dated to 1.509 ± 0.034 Ma (Kil-2-5).

3.2.2.2. The Acheulean Main Site (GqJh1) and Three-banded Tuff (3BT). The Acheulean Main Site GqJh 1 (Figs. 2 and 3) is exposed in an ancient broad shallow gully close to the top of the claystones. The Three-banded Tuff (3BT) (named by Bishop 1978) then occurs as a widespread marker on the eastern side of the trachyphonolite spur mentioned above. The 3BT is located about 1 m higher in the sequence than the main Acheulean archaeological horizon and comprises three tabular ash fallout layers, each approximately 30 cm thick.

The 3BT was previously suggested to record a reversed magnetic polarity, indicating that the main Acheulean site layer (GqJh1) was older than the age of the Brunhes-Matuyama boundary (Bishop 1978; Gowlett 1978). However, Dagley et al. (1978) were cautious on this point because the three samples were very strongly magnetised, and possibly represented an IRM induced by a lightning strike. The two samples from AH excavation were certainly reversed, but one from EH excavation gave a westerly direction. Our more recent measurements of the 3BT confirm that the high magnetisation, along with a reversed polarity, occurs at a number of different exposures of the 3BT spread over hundreds of metres. These findings indicate that the high magnetisation does not result from a lightning strike. The $^{40}Ar/^{39}Ar$ age from a sample of the 3BT taken from the main site area is 1.032 ± 0.025 Ma (Kil 2-2).

On the basis of the reversed polarity and the new $^{40}Ar/^{39}Ar$ age, the 3BT is likely to have formed shortly before or after the Jaramillo Subchron which extends from 1.072 to 0.988 Ma (Ogg, GTS2012, Chapter 5). Below the 3BT the archaeological horizons also record reversed magnetic polarity except for a layer at the very base of the Pale Pumiceous Tuff, which records normal polarity (Ashton, 2013). This change in polarity likely relates to the reversal at the end of the Jaramillo Subchron at 0.988 Ma. This would suggest that the 3BT and the main archaeological horizons are younger than the Jaramillo Subchron, with an age between the upper reversal of that subchron at 0.988 Ma and the younger limit on the age of date Kil-2-2 on the 3BT of 0.982 Ma. Within uncertainty, the $^{40}Ar/^{39}Ar$ age for this unit fits exactly and suggests that the 3BT was erupted very soon after the archaeological layer was deposited between 0.988 and 0.982 Ma. This age is similar to dates and correlations made for a tuff in Member 1 at Olorgesailie at 0.992 ± 0.39 Ma, which is also underlain by the upper Jaramillo reversal (Deino and Potts, 1990; Durkee and Brown, 2014). Durkee and Brown (2014) used correlations of volcanic ashes dating to 992-974 ka to refine the chronology of three other major Acheulean site complexes in Kenya – Olorgesailie, Isinya and Kariandusi (Isaac 1977; Potts et al., 1999; Gowlett and Crompton 1994; Texier 2018). The dates and their correlations suggest that the Kilombe main site (GqJh 1) (Figs. 2 and 3) is older than the Kariandusi sites, and the group of Acheulean sites in Member 7 of Olorgesailie (Isaac 1977), but of a similar age to the group of sites from Olorgesailie Member 1, and probably Isinya, which could however be somewhat younger (Sano et al., 2020). The site Garba XIII at Melka Kunturé also appears to be of similar age (Gallotti et al., 2014; Morgan et al., 2012). Work on other deposits at Kilombe and refinement of the polarity sequence is ongoing, including study of the fauna-bearing claystones underlying the main archaeological horizon, and the yellow tuff with grass prints (Bishop, 1978) mentioned above, now dated to 1.509 ± 0.034 Ma.

3.2.2.3. The Ash Flow Tuff. The three banded tuff is usually overlain by

around 15 m of reddish tuffaceous sediments (the Farmhouse Cliff Beds: Bishop 1978; Gowlett et al., 2015), capped by a brown, massive non-welded lapilli-ash tuff with thickness of some 7 m. The latter is a unit of the "Lower Menengai" Tuff series mapped by Jones (1975) (see also Jones and Lippard 1979), and like the 3BT, it is widespread in the area south of Kilombe mountain. According to Jones, to the SE, closer to Menengai caldera, the tuff units are developed with a great thickness of pumice which he states passes laterally into waterlain reworked tuff. Bombs within the pumice tuff become larger towards Menengai, indicating an origin from that source, rather than from Kilombe or Londiani volcanoes. The pumice-bearing unit is followed by the characteristic massive unwelded ash flow tuff (AFT) unit which is prominent in the Kilombe area. Main components are pumice clasts, compact obsidian and trachyte clasts, and feldspar crystals. Jones and Lippard (1979) describe it as 'a succession of pumiceous tuffs capped by an unwelded ignimbrite' (p. 699). As a resistant layer it has been largely responsible for the preservation of the underlying softer sediments. It is breached by erosion in the area of the Main Site (GqJh1), forming cliffs that face north into the Kibberenge valley. To the south it can be traced continuously into the valley of the Molo river, which it mantles. In sequences the AFT is usually the capping horizon, but in the area of Moricho 2 km to the west of Kilombe it is overlain by a succession of younger Middle Pleistocene sediments now also dated (see below).

The AFT has been dated at two places in the zone south of the mountain, both from the Farmhouse Cliff which overlooks the main site (GqJh1): Kil 1–3 is 0.461 ± 0.014 Ma and Kil 1–4 is 0.487 ± 0.011 Ma. At the 2-sigma confidence level these ages are indistinguishable and, taking into account the uncertainties, these samples define a weighted mean age for the AFT of 0.474 ± 0.009 Ma.

These deposits have a normal magnetic polarity, confirming that the AFT formed during the Brunhes Chron at <780 ka (Mark et al., 2017), consistent with its Middle Pleistocene $^{40}Ar/^{39}Ar$ age. Jones (1979) termed this marker "Lower Menengai" Tuff and mapped it as occurring within Kilombe caldera (as noted above).

Also within the Menengai assemblage is a trachyte, which was ^{40}K-^{40}Ar dated by Jones and Lippard (1979) from a trachyte boulder in Menengai caldera to ca. 0.30 Ma, although they commented on the unreliability of this age, and the context is also unverifiable. It was placed at the base of the Lower Menengai series, and was hitherto the only direct dating evidence available.

Leat (1984) argued that the AFT, visibly capping Farmhouse Cliff, was of Upper Pleistocene age, relating to a later eruption of Menengai thought to be at about 30 ka, and which has now been $^{40}Ar/^{39}Ar$ dated to ca. 36 ka by Blegen et al. (2016). Jones (1985) regarded Leat's interpretation as a misidentification, perhaps a confusion with later Menengai ashes which occur in the direction of Rongai. The stratigraphy at Moricho, the archaeology, and the new sequence of $^{40}Ar/^{39}Ar$ ages combine to show definitively the Middle Pleistocene age of the AFT. One or two Acheulean handaxes occur within the Farmhouse Cliff sediments as high as 1 m below the AFT: they would have an age of ca 0.5 Ma assuming a reasonable sedimentation rate, and are the youngest expressions of the Acheulean known in the area so far.

The new $^{40}Ar/^{39}Ar$ ages demonstrate that a major volcanic eruption,

Fig. 9. Sediments at Moricho site GqJh20, indicating the dated units 105, 104 and 103 (see text) exposed in a low outlier allowing investigation. Kilombe mountain is in the background.

Fig. 10. Top: bifacially worked flake and MSA bifacial point, both obsidian, from site GqJh20 dated to ~0.248–0.266 Ma. Below, two points from Site GqJh3 W 200; lower view is of casts showing greater surface detail. Scale in cm.

possibly on the scale of a caldera-forming event took place during the Middle Pleistocene, ca. 0.5 Ma. Jones (1975) on the basis of mapping close to Menengai mountain interpreted this as activity of a 'proto--Menengai', but there is also evidence of an eruption of Eburu volcano at a similar age (McCall 1967). In places surfaces of the AFT exposed by erosion may be overlain directly by a recent tuff, the Rongai black ash, mentioned by Bishop (1978), Jones (1975) and Jones and Lippard (1979).

3.3. Esageri Beds

Usually the AFT is present as a capping feature, as at Farmhouse Cliff, where it can be traced along two or 3 km of north-facing scarp. Further east, however, and to the west at Moricho, where there were lows in the ancient topography, the tuff is overlain by suites of younger sediments, mainly the Esageri Beds, the main component of Jones's Menengai assemblage (see Fig. 3, stratigraphic overview). At Moricho these are exposed in spectacular cliffs of 10–20 m height (Jennings 1971), fringing natural amphitheatres extending for more than 1 km along stream channels. They contain Middle Stone Age artefacts, including typical Levallois points of lava and obsidian, but usually the contexts of these cannot be defined because of the steepness of the exposures: the artefacts occur in scatters at the foot of the cliffs. In the area GqJh 20 (Figs. 2 and 9) a small low outlier of sediments was selected for archaeological investigation, as contamination from higher levels could be ruled out and the sediments are relatively accessible (Fig. 9). This area is a few metres above the AFT, although this is not locally visible, and three closely spaced tuffs have been dated from the lower part of this sequence. In ascending order the dates are 0.266 ± 0.003 Ma for Unit 105 (Kil-3-5), 0.275 ± 0.011 Ma for Unit 104 (Kil-3-4) and 0.248 ± 0.004 Ma for Unit 103 (Kil-3-3) (Table 1) (see Fig. 9).

The three tuffs are separated by thin layers of sediments containing MSA artefacts at the sampling point (Fig. 9). The pieces initially found included one small flake of obsidian, several flakes of lava, and a simple core on a cobble. Specimens found more recently confirm that bifacially worked obsidian points of MSA type occur within these levels (Fig. 10).

The finds occurred at low density in brown silty claystones which are very compacted. The tuffs are separated by ~2 m vertically (Fig. 9), suggesting that they reflect different volcanic events. When considering the uncertainty reported, the mean $^{40}Ar/^{39}Ar$ ages for Kil 3-3 and Kil 3–5 are indistinguishable. Together they place early Middle Stone Age evidence at ca. 250–265 ka. Similar ages are known for early MSA in the Baringo area, as well as at Olorgesailie (Johnson and McBrearty 2010; McBrearty 1999; Blegen 2017; Blegen et al., 2018; Deino et al., 2018; Brooks et al., 2018).

3.4. GqJh3 West area

The Esageri Beds were cut into by later incisional surfaces, visible at the north end of the Moricho exposures, and also apparent in the Kilombe (GqJh1) main site area (Bishop 1978). At the locality GqJh 3 West-200 (Fig. 2), about 1 km west of the main site area, and investigated from 2011, a long modern erosional 'amphitheatre' trending E-W exposes most of the local sequence in sections about 8 m high. Trachyphonolite is visible in places, overlain by brown claystones and then the Three banded Tuff. Above the 3BT is an unconformity (cutting out the 3BT at the eastern end of the exposures), and a succession of younger beds about 3 m thick. A thin yellow-brown tuff (Kil 2–7) in the in-fill is associated with *in situ* MSA artefacts (Fig. 10) and has been $^{40}Ar/^{39}Ar$ dated to 0.127 ± 0.030 Ma.

The artefacts at site 200 include long MSA points of obsidian (Hoare et al., 2020). The majority were found on the surface, but several obsidian flakes were recovered *in situ* just above and within the tuff. The $^{40}Ar/^{39}Ar$ age indicates that the incisional event and filling took place during the last interglacial *sensu lato* (MIS 5). A similar finding is supported by a further date of 0.111 ± 0.020 Ma (Kil-2-1) for a pale gritty-textured tuff occurring at the top of the fill of an incised feature on the main site GqJh1. It contains a few MSA artefacts in its basal layer.

The $^{40}Ar/^{39}Ar$ age is important for defining the continuation of Middle Stone Age human activity. Together with the $^{40}Ar/^{39}Ar$ age for the AFT and the early MSA, this places the neighbouring Moricho exposures within a bracket of ca. 0.47–0.12 Ma.

4. Discussion

The $^{40}Ar/^{39}Ar$ ages and stratigraphic settings detailed here represents a significant step forward in establishing a chronology for events in the central Kenyan Rift Valley, and also provides chronological resolution to archaeological sites or faunal localities at various points in the stratigraphic succession. In its two main parts, the described sequence provides a new major Pleistocene record.

The stratigraphic evidence, and the series of $^{40}Ar/^{39}Ar$ dates, coupled with the palaeomagnetic record, demonstrate that a major part of the Pleistocene is represented by volcanics and sediments forming Kilombe volcano, within its caldera (>100 m), and on its flanks (>50 m). The dating evidence has also established approximate chronostratigraphic relationships between the two areas of sedimentation within and outside Kilombe volcano. Archaeological traces are included within this record almost throughout its length, in at least ten discrete levels.

4.1. Significance of the Kilombe caldera-fill sequence

Although Early Pleistocene localities with fauna and/or hominin occupation have become more numerous in recent years, they remain sparse along much of the Central Rift Valley. Within the Baringo Basin they include Chemeron 70 km to the north in the Kapthurin area (Deino and Hill 2002; Deino et al., 2002; Sherwood et al., 2002), and the Chemoigut Formation on the eastern side of Lake Baringo at Chesowanja (Bishop et al. 1975, 1978; Gowlett et al., 1981). But Chemeron does not have archaeological sites, and Chemoigut is not established to date earlier than ~1.5 Ma. There is a gap of ca. 450 km to the north to the sites of East and West Turkana (Roche et al., 1999; Delagnes and Roche 2005; Harmand et al., 2015; Lepre et al., 2011; Isaac et al., 1997), and of 180 km to Kanam to the SW (Braun et al. 2009, 2010; Plummer and Bishop 2016; Plummer et al., 1999). Olduvai Gorge lies 350 km to the south (Leakey, 1975; Leakey and Roe, 1994; Deino 2012, Blumenschine et al., 2003, 2009, Blumenschine et al., 2012a, 2012b, Dominguez-Rodrigo et al., 2013; Diez-Martin et al., 2015; Uribelarrea et al., 2017; Stanistreet et al., 2020; Deino et al., 2020). The Kilombe caldera setting stands out from all these other sequences through its high altitude of around 2000 m – about 500 m more elevated than any other early East African archaeological locality (Olduvai Bed I is at 1400–1420 m, about 1500 m below the summit of neighbouring volcanoes Olmoti and Lemagrut), and perhaps even more important, it presents a steep and rugged landscape for which there has not previously been evidence of early hominin occupation from elsewhere in eastern Africa. The great majority of early Pleistocene hominin localities are preserved adjacent to lake, wetland or stream settings, all well away from the nearest major volcanic centres.

Biases in the representation of early sites on the landscape were made a focus of interpretation by Glynn Isaac (e.g. 1986). He noted the low likelihood of upland sites being preserved. More specific focuses on the issue have come from the work of Blumenschine and Peters at Olduvai, and from studies of tool transport at Kanam and Kanjera. Peters and Blumenschine (1995) examined land use potential around Olduvai, and in a succession of papers (e.g. Blumenschine and Peters 1998; Blumenschine et al., 2003, 2009, Blumenschine et al. 2012a, 2012b) sought to hypothesize and make tests of optimal and less optimal palaeoecologies and palaeoenvironments (affordances), in which early tool-making hominins (such as *Homo habilis*) would have exploited areas of the African Rift System and associated volcanic highlands, considering also their possible seasonal basis (Blumenschine and Peters 1998).

The Olduvai area was used as a test case, and it was deduced that optimal conditions would have been river-flanked areas high in the volcanic highlands, with access to fruits and rootstocks of those forested areas, as well as carcasses for scavenging. By contrast, settings more typically preserved geologically, and subsequently excavated archaeologically, tend to have been located at lower levels, where affordances for hominin exploitation were more ephemeral and marginal. At that time it was considered that environmental settings high on the volcano and its flanks were unlikely candidates for preservation.

The caldera setting at Kilombe, however, shows how a lacustrine sequence with fluvial and fan sequences prograding into a centrally situated lake can be preserved high on a volcano. A good modern analogue is Ngorongoro Caldera, which formed through major eruption and subsequent cauldron subsidence (Hay, 1976) ~2 Ma ago, and which still hosts saline-alkaline Lake Magadi with surrounding freshwater wetlands. Fan sedimentation proceeds off the caldera rim and fluvial input via the River Munge, provides analogue lateral settings where in the past hominins might have thrived.

Thus the occurrences discovered in the fill-sequence of Kilombe Caldera present an extremely rare opportunity to explore sites exploited by early hominins that were set in highlands, and potentially to contrast their archaeological characteristics with those in better-known lowland settings such as FLK Level 22 (Leakey, 1975; Blumenschine et al., 2012a; Dominguez-Rodrigo et al., 2007) and HWK E Level 1 (Leakey, 1975; Blumenschine et al., 2012b).

As of now artefacts are known from at least two stratigraphic zones in the caldera. The lower, dating to ~1.8 Ma, appears to have Oldowan characteristics in a generic sense. The presence in low numbers of choppers and flakes is entirely compatible with an Oldowan designation (cf. Hovers and Elias, 2012; Toth and Schick 2018). Currently locality GqJh13A has produced ~30 heavy-duty artefacts, including several choppers, heavy-duty scraper forms, and a discoid, as well as ~50 flakes and other debitage: Gowlett et al. in prep). Locally sourced trachyte appears to be the dominant raw material. It does not usually give high quality conchoidal fracture, but was adequate for providing robust sharp edges. The artefacts are found in a similar size-range to Olduvai Bed I (Leakey, 1975), with the core element appearing somewhat larger than tools characteristic of E. Turkana and Kanam (Isaac et al., 1997; Braun et al., 2009). Acheulean artefacts in some numbers come from a zone about 30 m higher in the sequence near the top of the Upper Staircase. They have been found *in situ* both on the surface embedded in sediment, and in step trenches. About 75 specimens have been found in total, including six bifaces or biface flakes. The date of the finds at the top of the Upper Staircase is not yet closely fixed, although they are younger than ~1.76 Ma. Like the Oldowan finds, they are made almost entirely of trachyte, without signs of the trachyphonolite that was widely used for bifaces outside the caldera, and which was deposited at ~1.56 Ma (see below). The specimens within the caldera could be older than this date, but further work is necessary to clarify this issue. The biface element includes both handaxes and biface flake blanks, with specimens up to 180 mm in length. They appear to have been entrained and redeposited within the mudflows, but without strong size-selection since some small elements are preserved, including a handaxe trimming flake.

4.2. Significance of the Kilombe mountain flank sequence

The southern mountain flank sequence includes Acheulean sites which have been known since the 1970s, but the new work greatly extends the sequence and improves its chronology. The dates for the trachyphonolite lava establish a base of ca 1.57 Ma for the main Kilombe sequence on the flanks of the mountain – shared approximately with basal dates for the Kapthurin Formation at Baringo, Kenya (Deino and McBrearty 2002). As the earliest dates obtained for the Acheulean in East Africa are older than this (e.g. West Turkana, Konso Gardula, and Olduvai (Lepre et al., 2011; Beyene et al., 2013, 2015; de la Torre, 2016; Diez-Martín et al., 2015, Gallotti 2013; Gallotti and Mussi 2017), an Acheulean presence would be possible even down to the base of the southern flank sequence in the Kilombe area, but outside the caldera no Acheulean traces have yet been found at levels lower than the main site (GqJh1, Figs. 2 and 5), now dated to ~1.0. Ma.

The extensive Acheulean of the Main Site (GqJh1) thus remains the oldest at Kilombe outside the caldera. Its date of around 1.0 Ma is very close to that for Kariandusi, 80 km to the SE (Durkee and Brown 2014; Gowlett 1980; Gowlett and Crompton 1994). Dates at Kariandusi appear to be slightly under one million years for the Upper Site localities containing many obsidian handaxes, and certainly >~0.8 Ma on the basis of the palaeomagnetic evidence. In a tuff correlation study Durkee and Brown (2014) argued for a similar date for Isinya, although this is queried by Sano et al. (2020), while the oldest dates for the Olorgesailie Formation, just above the artefact horizons of Member 1, are also around 0.974–0.992 Ma (Durkee and Brown 2014; Isaac 1977; Potts et al., 1999). These dates coincide with a long-lasting wet phase in the Rift Valley emphasized by Trauth et al. (2005).

The central Rift Valley region in Kenya provides very rare opportunities for comparing *penecontemporaneous* Acheulean assemblages (cf Isaac 1977; Gowlett 2015). At Kilombe itself, the stratigraphic range of the Acheulean established so far is from the main horizon below the 3BT up to a point immediately below the AFT – covering a period of about 0.5 million years. Metrical and morphological comparisons are possible between the main horizon and two sets of bifaces from the Farmhouse Cliff sediments: around 20 bifaces from Kilombe GqJh3 West (KW) come from layers up to 5 m above the three banded tuff, and so somewhat lower than another set from the northeastern gullies (Fig. 2, Kilombe GqJh2 South NE). These last correlate with higher levels of the Farmhouse Cliff sediments, close to the position of the Brunhes-Matuyama boundary. The comparisons of bifaces made so far suggest that the basic pattern of Kilombe bifaces generally made of trachyphonolite, and having a mean length of ca. 150 mm, was maintained between 1 million years and the B/M boundary 200 ka later without obvious change (Gowlett 2015). A similar pattern may be maintained because of the use of the same raw materials, perhaps encouraging a similar mean size of the large flakes used as biface blanks (cf., Sharon 2007).

The AFT has importance as a stratigraphic marker, and also potentially has great use chronostratigraphically, as its time point of 0.474 ± 0.009 Ma is in a range often difficult to date at high resolution in archaeological sequences except when $^{40}Ar/^{39}Ar$ geochronology can be applied. Boxgrove in Britain is one of the few sites that can be pinned to this period outside Africa (Roberts and Parfitt 1999; Pope and Roberts 2005). There is, however, widespread interest in the dating of technological changes which may begin from around this time in Africa, and which culminate eventually in expressions of the MSA (e.g. Barham 2013; Basell 2008; Blome et al., 2012; Brooks et al., 2018; McBrearty and Brooks 2000; Pleurdeau 2006; Wendorf and Schild 1974). Johnson and McBrearty (2010) highlight the early presence of stone blades at Kapthurin at this time, and according to Wilkins et al. (2012), major technological change can also be detected from this period at Kathu Pan in southern Africa, where projectile points suitable for hafting were dated by use of OSL on sediments. On the Kilombe southern flanks the Acheulean occurs very sporadically in the upper part of the levels between the Main Site (GqJh1) and the AFT. One handaxe was found just 1 m below the tuff, just north of GqJh2 (Fig. 8). Also in GqJh2 area, a double-pointed biface was found, close to the AFT level. This distinctive form is reminiscent of later Lupemban forms, but can also be matched by one earlier example from Olorgesailie (Isaac 1977, Figure 73, p.221). Until now no handaxes have been found above the AFT, although the lower levels at Moricho at ~280-250 ka are demonstrably within a time-range where both Middle Stone Age and late Acheulean facies might be found. The fullest sequences for comparison are Kapthurin, 70 km to the north and Olorgesailie, 180 km to the south. At Kapthurin an Acheulean industry with Levallois flakes occurs as young as ~0.4 Ma, but MSA features are also evident around this time, and in industries with transported obsidian before ~200 ka (Blegen et al., 2018;

McBrearty 1999; Tryon 2006; Tryon and McBrearty 2002, 2006); at Olorgesailie from the same period similar occurrences of both Acheulean-like and MSA industries are found (Brooks et al., 2018; Deino et al., 2018), and the Moricho finds appear consistent with this picture, although the zone immediately above the AFT is not easily accessible for investigation.

The upper sequence around Kilombe is complex. There was further sedimentation above the AFT, especially in depressions, as at Moricho to the west of Kilombe, and to the east of the trachyphonolite spur where the small Kibberenge valley descends parallel to the River Molo (Fig. 2). These are the thick red beds noted by Jennings (1971) and named by Jones (1975) as the Esageri Beds. Channels, sometimes containing tuffs in their fill, cut into the upper levels of these beds, both at Moricho and at Kilombe. The most important locality to date occurs about halfway between Moricho and Kilombe, 2 km west of the Kilombe Main Site (GqJh1). This is the Middle Stone Age locality of Kilombe GqJh3 West 200 (Hoare et al., 2020), now dated to 127 ± 30 ka. The date of 111 ± 20 ka from the main site GqJh1 confirms sedimentary events and human presence at about the same time. Geochemical analysis undertaken on obsidian points from this locality suggests the use of multiple sources and the long-distance transportation of high-quality obsidian from over 80 km away in MIS 5. The outline sequence of Middle Stone age localities presented here is now relatively well-dated, but more work will be needed to elaborate it archaeologically. Artefacts, mainly of obsidian, occur at low density in the known localities. Where there are denser obsidian scatters, they tend to have accumulated at the base of steep cliffs, making further exploration challenging. There are however places where overlying levels have been eroded away, and the relevant localities are more accessible. The finds already add to the regional picture of a MSA deeply established in time (Basell 2008), probably from around 300 ka, and with transport of obsidian materials from distant sources, as established by Blegen et al. (2016) at Baringo.

5. Conclusion

The new investigations across Kilombe volcano, on its flanks and within its caldera, coupled with the palaeomagnetic evidence and a series of new $^{40}Ar/^{39}Ar$ dates, demonstrate a major new sequence of lava flows and tuffs, fluvio-lacustrine sedimentation and archaeology ranging through almost the entire Pleistocene. It is one of the more complete of such sequences, and the only one which was generated in a highland context, significantly demonstrating early hominin presence at highpoints in the rugged landscape. The dates confirm that the major feature of the landscape, Kilombe volcano itself, assumed something like its present shape ~2.5 Ma years ago. Bedded tuffs and lake sediments accumulated within its caldera and evidently, at times between eruptions, the area surrounding an intra-caldera lake presented an attractive environment to animals. These included large mammals such as hippopotamus (the extinct *Hippopotamus gorgops*) found in new faunal localities of an age corresponding to Olduvai Bed I. The presence of early artefacts at multiple localities proves for the first time that early hominins regularly exploited these topographically upland settings.

The lack of trachyphonolite artefacts within the caldera might indicate that Acheulean artefacts there are likely to be older than those known outside the mountain, but further research is required to test this point.

The Acheulean occurrences on the lower flanks of the mountain are now documented to occur through most of the time range 1.0–0.5 Ma. The oldest remain those of the Main Site (GqJh1), about 1 m below the approximately million-year-old Three-banded Tuff (3BT); the youngest, immediately below the Ash Flow Tuff (AFT), is around half that age. The AFT represents a cataclysmic eruption in the area, probably from the Menengai direction, and it, together with its underlying unconformity surface provides a benchmark for chronostratigraphic studies in the region. Further work will be needed to determine a full chronology for the later Middle to Upper Pleistocene deposits of Moricho and Kilombe overlying the AFT, but key points are already established, through the dates for early MSA sites in the range ~250–270 ka at Moricho (Figs. 2 and 3), and in the date for the Middle Stone Age MSA site GqJh3W-200, which belongs to the beginning of the Upper Pleistocene, approximately 120,000 years ago. Later Stone Age surface sites complete the sequence.

Above all, the Kilombe sedimentary archive records the repeated presence of early humans in the one area. The evidence from Kilombe mountain includes traces of well-watered environments at several times in the past, with hippopotamus featuring in at least three levels. Early and later hominins may have exploited these environments in the repeated way that we observe partly because of the ecotonal aspect that a variety of resources were available within a few kilometres at very different altitudes. The Kilombe record therefore now provides exceptional opportunities for further research on landscape and its varied use by hominins through the entire duration of the Pleistocene.

Declaration of competing interest

None.

Acknowledgments

Fieldwork support has been received from The Leverhulme Trust grant [RPG-2017-183], PAST Foundation, Wenner-Gren Foundation [Gr. 9536], and a British Academy-supported Mobility and Links Project between University of Liverpool and National Museums of Kenya (2013–2016). The dating work was supported by NERC awards IP-354-1112 and IP-1617-0516. NERC are thanked for continued support of the $^{40}Ar/^{39}Ar$ facility at SUERC. JAJG is grateful for support from the British Academy Centenary Project, and help and permissions from NACOSTI and National Museums of Kenya. SH is grateful for support from the AHRC (PhD studentship) and NERC and SUERC. AH acknowledges funding from the Australian Research Council via Future Fellowship FT 120100399. Thanks are owed to Willy Jones, Laura Basell, Fabienne Marret-Davies, Darren Curnoe, Robin Crompton, Stephen Lycett, Ginette Warr, Sian Davies, Mimi Hill and Natalie Uomini; our colleagues R.M. Albert, C. Komboh, R. Muthoni; to the Commissioner for Baringo County, Mr H. Wafula; and our Kenyan helpers at Kilombe caldera, especially Mr Philip Kogai. We also thank Maura Butler; and those who are still missed: Jean-Claude (J.C.) Tubiana, Bill Bishop, and our colleague and co-author James Brink.

Appendix A. Supplementary data

Supplementary data to this article can be found online at https://doi.org/10.1016/j.jas.2020.105273.

References

Ashton, R., 2013. Palaeomagnetic Analysis and Age Estimate of the Kilombe Acheulian and Fossil Bearing Deposits. Kenya. Unpublished honours thesis. Dept. Archaeology, La Trobe University, Australia.

Barham, L., 2013. From Hand to Handle: the First Industrial Revolution. Oxford University Press, Oxford.

Basell, L.S., 2008. Middle Stone Age (MSA) site distributions in eastern Africa and their relationship to Quaternary environmental change, refugia and the evolution of *Homo sapiens*. Quat. Sci. Rev. 27, 2484–2498.

Beyene, Y., Katoh, S., WoldeGabriel, G., Hart, W.K., Uto, K., Kondo, M., Hyodo, M., Renne, P.R., Suwa, G., Asfaw, B., 2013. The characteristics and chronology of the earliest Acheulean at Konso, Ethiopia. Proc. Natl. Acad. Sci. U.S.A. 110, 1584–1591. https://doi.org/10.1073/pnas.1221285110.

Beyene, Y., Asfaw, B., Sano, K., Suwa, G., 2015. Konso-gardula research project volume 2: archaeological collections: background and the early acheulean assemblages. Bulletin, 48. the University Museum, the University of Tokyo, Tokyo.

Bishop, W.W., 1978. Geological framework of the Kilombe Acheulian site, Kenya. In: Bishop, W.W. (Ed.), Geological Background to Fossil Man. Scottish Academic Press, Edinburgh, pp. 329–336.

Bishop, W.W., Hill, A., Pickford, M., 1978. Chesowanja: a revised geological interpretation. In: Bishop, W.W. (Ed.), Geological Background to Fossil Man. Scottish Academic Press, Edinburgh, pp. 309–328.

Bishop, W.W., Pickford, M., Hill, A., 1975. New evidence regarding the Quaternary geology, archaeology, and hominids of Chesowanja, Kenya. Nature 258, 204–208.
Blegen, N., 2017. The earliest long-distance obsidian transport: evidence from the ~200 ka Middle Stone Age Sibilo School Road site, Baringo, Kenya. J. Hum. Evol. 103, 1–19.
Blegen, N., Brown, F.H., Jicha, B.R., Binetti, K.M., Faith, J.T., Ferraro, J.V., Gathogo, P. N., Richardson, J.L., Tryon, C.A., 2016. The Menengai Tuff: a 36 ka widespread tephra and its chronological relevance to Late Pleistocene human evolution in East Africa. Quat. Sci. Rev. 152, 152–168.
Blegen, N., Jicha, B.R., McBrearty, S., 2018. A new tephrachronology for early diverse stone tool technologies and long-distance raw material transport in the Middle to Late Pleistocene Kapthurin formation, East Africa. J. Hum. Evol. 121, 75–103.
Blome, M.W., Cohen, A.S., Tryon, C.A., Brooks, A.S., Russell, J., 2012. The environmental context for the origins of modern human diversity: a synthesis of regional variability in African climate 150,000–30,000 years ago. J. Hum. Evol. 62, 563–592.
Blumenschine, R.J., Masao, F.T., Stollhofen, H., Stanistreet, I.G., Bamford, M.K., Albert, R.M., Njau, J.K., Prassack, K.A., 2012a. Landscape distribution of Oldowan stone artifact assemblages across the fault compartments of the eastern Olduvai Lake Basin during early lowermost Bed II times. Five Decades after *Zinjanthropus* and *Homo habilis*: Landscape Paleoanthropology of Plio-Pleistocene Olduvai Gorge, Tanzania J. Hum. Evol. 63 (2), 384–394.
Blumenschine, R.J., Peters, C.R., 1998. Archaeological predictions for hominid land use in the paleo-Olduvai Basin, Tanzania, during lowermost Bed II times. J. Hum. Evol. 34, 565–607.
Blumenschine, R.J., Peters, C.R., Masao, F.T., Clarke, R.J., Deino, A.L., Hay, R.L., Swisher, C.C., Stanistreet, I.G., Ashley, G.M., McHenry, L.J., Sikes, N.E., van der Merwe, N.J., Tactikos, J.C., Cushing, A.E., Deocampo, D.M., Njau, J.K., Ebert, J.I., 2003. Late Pliocene *Homo* and hominid land use from western Olduvai Gorge, Tanzania. Science 299, 1217–1221.
Blumenschine, R., Masao, F.T., Stanistreet, I.G., 2009. Changes in hominin transport of stone tools across the eastern Olduvai Basin during lowermost Bed II times. In: Schick, K., Toth, N. (Eds.), The cutting edge: new approaches to the Archaeology of Human Origins. Stone Age Institute Press, Gosport, pp. 1–15.
Braun, D., Plummer, T.W., Ferraro, J., Ditchfield, P., Bishop, L., 2009. Raw material quality and Oldowan hominin toolstone preferences: evidence from Kanjera South. J. Archaeol. Sci. 36, 1605–1614.
Blumenschine, R.J., Stanistreet, I.G., Njau, J.K., Bamford, M.K., Masao, F.T., Albert, R. M., Stollhofen, H., Andrews, P., Prassack, K.A., McHenry, L.J., Fernandez-Jalvo, Y., Camilli, E.L., Ebert, J.I., 2012b. Environments and activity traces of hominins across the FLK peninsula during *Zinjanthropus* times (1.84 Ma), Olduvai Gorge, Tanzania. Five Decades after *Zinjanthropus* and *Homo habilis*: Landscape Paleoanthropology of Plio-Pleistocene Olduvai Gorge, Tanzania J. Hum. Evol. 63 (2), 364–383.
Braun, D.R., Harris, J.W.K., Levin, N.E., McCoy, J.T., Herries, A.I.R., Bamford, M.K., Bishop, L.C., Richmond, B.G., Kibunjia, M., 2010. Early hominin diet included diverse terrestrial and aquatic animals 1.95 Ma in East Turkana, Kenya. Proc. Natl. Acad. Sci. U.S.A. 107, 10002–10007.
Brooks, A.S., Yellen, J.E., Potts, R., Behrensmeyer, A.K., Deino, A.L., Leslie, D.E., Ambrose, S.H., Ferguson, J.R., d'Errico, F., Zipkin, A.M., Whittaker, S., Post, J., Veatch, E.G., Foecke, K., Clark, J.B., 2018. Long-distance stone transport and pigment use in the earliest Middle Stone Age. Science 360, 90–94. https://doi.org/10.1126/science.aao2646.
Dagley, P., Mussett, A.E., Palmer, H.C., 1978. Preliminary observations on the palaeomagnetic stratigraphy of the area west of Lake Baringo, Kenya. In: Bishop, W. W. (Ed.), Geological Background.to Fossil Man. Scottish Academic Press, Edinburgh, pp. 225–236.
de la Torre, I., 2016. The origins of the Acheulean: past and present perspectives on a major transition in human evolution. Phil. Trans. R. Soc. B 371, 20150245. https://doi.org/10.1098/rstb.2015.0245.
Deino, A.L., 2012. $^{40}Ar/^{39}Ar$ dating of Bed I, Olduvai Gorge, Tanzania, and the chronology of early Pleistocene climate change. J. Hum. Evol. 63, 251–273. https://doi.org/10.1016/j.jhevol.2012.05.004.
Deino, A.L., Hill, A., 2002. $^{40}Ar/^{39}Ar$ dating of the Chemeron Formation strata encompassing the site of hominid KNM-BC 1, Tugen Hills, Kenya. J. Hum. Evol. 42, 141–151.
Deino, A.L., McBrearty, S., 2002. $^{40}Ar/^{39}Ar$ dating of the Kapthurin Formation, Baringo, Kenya. J. Hum. Evol. 42, 185–210. https://doi.org/10.1006/jhev.2001.0517.
Deino, A.L., Tauxe, L., Monaghan, M., Hill, A., 2002. $^{40}Ar/^{39}Ar$ geochronology and paleomagnetic stratigraphy of the Lukeino and Lower Chemeron succession at Tabarin and Kapcheberek, Tugen Hills, Kenya. J. Hum. Evol. 42, 117–140.
Deino, A.L., Behrensmeyer, A.K., Brooks, A.S., Yellen, J.E., Sharp, W.D., Potts, R., 2018. Chronology of the Acheulean to Middle Stone Age transition in eastern Africa. eaao2216 Science. https://doi.org/10.1126/science.aao2216.
Deino, A.L., Heil, C. Jr., King, J., McHenry, L.J., Stanistreet, I.G., Stollhofen, H., Njau, J. K., Mwankunda, J., Schick, K.D., Toth, N., 2020. Chronostratigraphy and age modeling of Quaternary drill cores from the Olduvai basin, Tanzania (Olduvai Gorge coring project). Palaeogeogr. Palaeoclimatol. Palaeoecol. In press.
Delagnes, A., Roche, H., 2005. Late Pliocene hominid knapping skills: the case of Lokalalei 2C, West Turkana, Kenya. J. Hum. Evol. 48, 435–472.
Diez-Martín, F., Yustos, P.S., Uribelarrea, D., Baquedano, E., Mark, D.F., Mabulla, A., Fraile, C., Duque, J., Díaz, I., Pérez-González, A., Yravedra, J., 2015. The origin of the Acheulean: the 1.7 million-year-old site of FLK West, Olduvai Gorge (Tanzania). Dec 7 Sci. Rep. 5 (17839). https://doi.org/10.1038/srep17839.
Domínguez-Rodrigo, M., Barba, R., Egeland, C., 2007. Deconstructing Olduvai: a Taphonomic Study of the Bed I Sites. Springer, Dordrecht.
Domínguez-Rodrigo, M., Pickering, T.R., Baquedano, E., Mabulla, A., Mark, D.F., Musiba, C., Bunn, H.T., Uribelarrea, D., Smith, V., Diez-Martin, F., Pérez-González, A., Sánchez, P., Santonjaa, M., Barboni, D., Gidna, A., Ashley, G., Yravedra, J., Heaton, J.L., Arriaza, M.C., 2013. First partial skeleton of a 1.34-million-year-old *Paranthropus boisei* from bed II, Olduvai Gorge, Tanzania. PloS One 8, e80347.
Durkee, H., Brown, F.H., 2014. Correlation of volcanic ash layers between the early Pleistocene Acheulean sites of Isinya, Kariandusi, and Olorgesailie, Kenya. J. Archaeol. Sci. 49, 510–517.
Gallotti, R., 2013. An older origin for the Acheulean at Melka Kunture (Upper Awash, Ethiopia): techno-economic behaviors at Garba IVD. J. Hum. Evol. 65, 594–620.
Gallotti, R., Mussi, M., 2017. Two Acheuleans, two humankinds: from 1.5 to 0.85 Ma at Melka Kunture (Upper Awash, Ethiopian highlands). J. Anthropol. Sci. 95, 1–46.
Gallotti, R., Raynal, J.-P., Geraads, D., Mussi, M., 2014. Garba XIII (Melka Kunture, Upper Awash, Ethiopia): a new Acheulean site of the late Lower Pleistocene. Quat. Int. 343, 17–27.
Gowlett, J.A.J., 1978. Kilombe - an Acheulian site complex in Kenya. In: Bishop, W.W. (Ed.), Geological Background to Fossil Man. Scottish Academic Press, Edinburgh, pp. 337–360.
Gowlett, J.A.J., 1980. Acheulean sites in the central Rift valley, Kenya. In: Leakey, R.E., Ogot, B.A. (Eds.), *Proceedings of the 8th Panafrican Congress of Prehistory and Quaternary Studies, Nairobi,1977*. TILLMIAP, Nairobi, pp. 213–217.
Gowlett, J.A.J., 1993. Le site Acheuléen de Kilombe: stratigraphie, géochronologie, habitat et industrie lithique. L'Anthropologie 97 (1), 69–84.
Gowlett, J.A.J., 2015. Variability in an early hominin percussive tradition: the Acheulean versus cultural variation in modern chimpanzee artefacts. Phil. Trans. R. Soc. B 370, 20140358. https://doi.org/10.1098/rstb.2014.0358.
Gowlett, J.A.J., 2020. Deep Structure in the Acheulean adaptation: technology, sociality and aesthetic emergence. Adapt. Behav. https://doi.org/10.1177/1059712320965713.
Gowlett, J.A.J., Crompton, R.H., 1994. Kariandusi: Acheulean morphology and the question of allometry. Afr. Archaeol. Rev. 12, 3–42.
Gowlett, J.A.J., Brink, J.S., Herries, A.I.R., Hoare, S., Rucina, S.M., 2017. The small and short of it: mini-bifaces and points from Kilombe, Kenya, and their place in the Acheulean. In: Wojtczak, D., Al Najjar, M., Jagher, R., Elsuede, H., Wegmüller, F. (Eds.), Vocation Préhistoire: Homage à Jean-Marie Le Tensorer, vol. 148. ERAUL, Liège, pp. 121–132.
Gowlett, J.A.J., Brink, J.S., Herries, A.I.R., Hoare, S., Onjala, I., Rucina, S.M., 2015. At the heart of the African Acheulean: the physical, social and cognitive landscapes of Kilombe. In: Coward, F., Hosfield, R., Wenban-Smith, F. (Eds.), Settlement, Society and Cognition in Human Evolution: Landscapes in Mind. Cambridge University Press, Cambridge, pp. 75–93.
Gowlett, J.A.J., Harris, J.W.K., Walton, D., Wood, B.A., 1981. Early archaeological sites, hominid remains and traces of fire from Chesowanja, Kenya. Nature 294, 125–129.
Griffiths, P.S., Gibson, I.L., 1980. The geology and petrology of the Hannington Trachyphonolite Formation, Kenya rift valley. Lithos 13, 43–53.
Harmand, S., Lewis, J.E., Feibel, C.S., Lepre, C.J., Prat, S., Lenoble, A., Boës, A., Quinn, R. L., Brenet, M., Arroyo, A., et al., 2015. 3.3-million-year-old stone tools from Lomekwi 3, West Turkana, Kenya. Nature 521, 310–315.
Hay, R.L., 1976. Geology of the Olduvai Gorge. University of California Press, Berkeley.
Herries, A.I.R., Davies, S., Brink, J., Curnoe, D., Warr, G., Hill, M., Rucina, S., Onjala, I., Gowlett, J.A.J., 2011. New explorations and magnetobiostratigraphical analysis of the Kilombe Acheulian localitiy, central Rift, Kenya. PaleoAnthropology 2011, A16.
Hoare, S., Rucina, S., Gowlett, J.A.J., 2020. Initial source evaluation of archaeological obsidian from Middle Stone Age site GqJh3 West 200. In: Cole, J., McNabb, J., Grove, M., Hosfield, R. (Eds.), Landscapes of Human Evolution: Contributions in Honour of John Gowlett. Archaeopress, Oxford, pp. 142–149.
Hovers, E., 2012. Invention, reinvention and innovation: the makings of Oldowan lithic technology. In: Elias, S. (Ed.), Origins of Human Innovation and Creativity. In: van der Meer, J.J.M. (Ed.), *Developments In Quaternary Science* 16. Elsevier B.V., pp. 51–68
Isaac, G.Ll, 1977. Olorgesailie: Archaeological Studies of a Middle Pleistocene Lake Basin in Kenya. University of Chicago Press, Chicago.
Isaac, G. Ll, 1986. Foundation stones: early artefacts as indicators of activities and abilities. In: Bailey, G.N., Callow, P. (Eds.), Stone Age Prehistory: Studies in Memory of Charles McBurney. Cambridge University Press, Cambridge, pp. 221–241.
Isaac, G.Ll, Harris, J.W.K., Kroll, E.M., 1997. The stone artefact assemblages: a comparative study. In: Isaac, G.Ll, Isaac, B. (Eds.), Koobi Fora Research Project Volume 5: Plio-Pleistocene Archaeology. Clarendon Press, Oxford, pp. 262–362.
Jennings, D.J., 1971. Geology of the Molo area. Ministry of Natural Resources, Geological Survey of Kenya. Report No. 86.
Johnson, S.R., McBrearty, S., 2010. 500,000 year-old blades from the Kapthurin Formation, Kenya. J. Hum. Evol. 58, 193–200.
Jones, W.B., 1975. The Geology of the Londiani Area of the Kenya Rift Valley. Unpublished PhD thesis, Univ, London.
Jones, W.B., 1985. Discussion on the geological evolution of the trachyte caldera volcano Menengai, Kenya Rift Valley. London J. Geol. Soc. 142, 711–712.
Jones, W.B., 1988. Listric growth faults in the Kenya rift valley. J. Struct. Geol. 10, 661–672.
Jones, W.B., Lippard, S.J., 1979. New age determinations and geology of the Kenya Rift-Kavirondo Rift junction, W. Kenya. London J. Geol. Soc. 136, 693–704.
Kuiper, K.F., Deino, A., Hilgen, F.J., Krijgsman, W., Renne, P.R., Wijbrans, J.R., 2008. Synchronizing rock clocks of Earth history. Science 320 (5875), 500–504.
Leakey, M.D., 1975. Cultural patterns in the Olduvai sequence. In: Butzer, K.W., Isaac, G. Ll (Eds.), After the Australopithecines. Mouton, The Hague, pp. 477–494.

Leakey, M.D., Roe, D.A. (Eds.), 1994. Olduvai Gorge, Volume 5: Excavations in Beds III, IV and the Masek Beds, 1968-1971. Cambridge University Press, Cambridge.
Leat, P.T., 1984. Geological evolution of the trachyte caldera volcano Menengai, Kenya Rift Valley. London J. Geol. Soc. 141, 1057–1069.
Lee, J.Y., Marti, K., Severinghaus, J.P., Kawamura, K., Yoo, H.S., Lee, J.B., Kim, J.S., 2006. A redetermination of the isotopic abundances of atmospheric Ar. Geochem. Cosmochim. Acta 70 (17), 4507e4512.
Lepre, C.J., Roche, H., Kent, D.V., Harnand, S., Quinn, R.L., Brugal, J.-P., Texier, P.-J., Feibel, C.S., 2011. An earlier origin for the Acheulian. Nature 477, 82–85. https://doi.org/10.1038/nature10372.
McBrearty, S., 1999. The archaeology of the Kapthurin Formation. In: Andrews, P., Banham, P. (Eds.), Late Cenozoic Environments and Hominid Evolution: a Tribute to Bill Bishop. Geological Society, London, pp. 143–156.
McBrearty, S., Brooks, A.S., 2000. The revolution that wasn't: a new interpretation of the origin of modern human behavior. J. Hum. Evol. 39, 453–563.
McCall, G.J.H., 1964. Kilombe caldera, Kenya. Proc. Geologists' Assoc. 75, 563–572.
McCall, G.J.H., 1967. *Geology of the Nakuru-Thomson's falls-Lake Hannington area*. Ministry of Natural Resources, Geological Survey of Kenya. Report No. 78.
Mark, D.F., Gonzalez, S., Huddart, D., Böhnel, H., 2010. Dating of the Valsequillo volcanic deposits: resolution of an ongoing archaeological controversy in Central Mexico. J. Hum. Evol. 58 (5), 441–445.
Mark, D.F., Stuart, F.M., de Podesta, M., 2011. New high-precision measurements of the isotopic composition of atmospheric argon. Geochem. Cosmochim. Acta 75 (23), 7494–7501.
Mark, D.F., Petraglia, M., Smith, V.C., Morgan, L.E., Barfod, D.N., Ellis, B.S., Pearce, N.J., Pal, J.N., Korisettar, R., 2014. A high-precision $^{40}Ar/^{39}Ar$ age for the Young Toba Tuff and dating of ultra-distal tephra: forcing of Quaternary climate and implications for hominin occupation of India. Quat. Geochronol. 21, 90–103.
Mark, D.F., Renne, P.R., Dymock, R., Smith, V.C., Simon, J.I., Morgan, L.E., Staff, R.A., Ellis, B.S., Pearce, N.J.G., 2017. High precision $^{40}Ar/^{39}Ar$ dating of Pleistocene tuffs and temporal anchoring of the Matuyama-Brunhes boundary. Quat. Geochronol. 39, 1–23.
Morgan, L.E., Renne, P.R., Kieffer, G., Piperno, M., Gallotti, R., Raynal, J.-P., 2012. A chronological framework for a long and persistent archaeological record: Melka Kunture, Ethiopia. J. Hum. Evol. 62, 104–115. https://doi.org/10.1016/j.jhevol.2011.10.007.
Niespolo, E.M., Rutte, D., Deino, A.L., Renne, P.R., 2017. Intercalibration and age of the Alder Creek sanidine $^{40}Ar/^{39}Ar$ standard. Quat. Geochronol. 205–213.
Peters, C.R., Blumenschine, R.J., 1995. Landscape perspectives on possible land use patterns for early hominids in the Olduvai Basin. J. Hum. Evol. 29, 321–362.
Pleurdeau, D., 2006. Human technical behavior in the African Middle Stone Aage: the lithic assemblage of Porc-Epic cave (Dire Dawa, Ethiopia). Afr. Archaeol. Rev. 22, 177–197.
Plummer, T.W., Bishop, L.C., 2016. Oldowan hominin behaviour at Kanjera South, Kenya. J. Anthropol. Sci. 94, 29–40.
Plummer, T., Bishop, L.C., Ditchfield, P., Hicks, J., 1999. Research on late Pliocene Oldowan sites at Kanjera South, Kenya. J. Hum. Evol. 36, 151–170.
Pope, M.I., Roberts, M.B., 2005. Observations on the relationship between Palaeolithic individuals and artefact scatters at the Middle Pleistocene site of Boxgrove, UK. In: Gamble, C.S., Porr, M. (Eds.), The Hominid Individual in Context: Archaeological Investigations of Lower and Middle Palaeolithic, Landscapes, Locales and Artefacts. Routledge, London, pp. 81–97.
Potts, R., Behrensmeyer, A.K., Ditchfield, P., 1999. Paleolandscape variation and early Pleistocene hominid activities: members 1 and 7, Olorgesailie Formation, Kenya. J. Hum. Evol. 37, 747–788.
Renne, P.R., 2014. Some footnotes to the optimization-based calibration of the $^{40}Ar/^{39}Ar$ system, 378. Geological Society of London Special Publication, 21-31.
Renne, P.R., Cassata, W.S., Morgan, L.E., 2009. The isotopic composition of atmospheric argon and $^{40}Ar/^{39}Ar$ geochronology: time for a change? Quat. Geochronol. 4 (4), 288–298.
Renne, P.R., Norman, E.B., 2001. Determination of the half-life of ^{37}Ar by mass spectrometry. Phys. Rev. C 63 (4), 047302.
Renne, P.R., Mundil, R., Balco, G., Min, K., Ludwig, K.R., 2011. Response to the comment by W. H. Schwarz et al. on "Joint determination of ^{40}K decay constants and $^{40}Ar^*/^{40}K$ for the Fish Canyon sanidine standard, and improved accuracy for $^{40}Ar/^{39}Ar$ geochronology". Geochem. Cosmochim. Acta 75, 5097-5100.
Renne, P.R., Mundil, R., Balco, G., Min, K., Ludwig, K.R., 2010. Joint determination of ^{40}K decay constants and $^{40}Ar^*/^{40}K$ for the Fish Canyon sanidine standard, and improved accuracy for $^{40}Ar/^{39}Ar$ geochronology. Geochem. Cosmochim. Acta 74 (18), 5349–5367.
Renne, P.R., Sharp, Z.D., Heizler, M.T., 2008. Cl-derived argon isotope production in the CLICIT facility of OSTR reactor and the effects of the Cl-correction in $^{40}Ar/^{39}Ar$ geochronology. Chem. Geol. 255 (3e4), 463–466.
Ridolfi, F., Renzulli, A., Macdonald, R., Upton, B.G.J., 2006. Peralkaline syenite autoliths from Kilombe volcano, Kenya Rift Valley: evidence for subvolcanic interaction with carbonatitic fluids. Lithos 91, 373–392.
Riedl, S., Melnick, D., Mibei, G.K., Njue, L., Strecker, M.R., 2020. Continental rifting at magmatic centres: structural implications from the Late Quaternary Menengai caldera, central Kenya rift. J. Geol. Soc. 177, 153–169.
Roberts, M.B., Parfitt, S.G., 1999. Boxgrove: A Middle Pleistocene Hominid Site at Eartham Quarry. Boxgrove, West Sussex. English Heritage, London.
Roche, H., Delagnes, A., Brugal, J.-P., Feibel, C., Kibunjia, M., Mourre, V., Texier, J.-P., 1999. Early hominid stone tool production and technical skill 2.34 Myr ago in West Turkana, Kenya. Nature 399, 57–60.
Sano, K., Beyene, Y., Katoh, S., Koyabu, D., Endo, H., Sasaki, T., Asfaw, B., Suwa, G., 2020. A 1.4-million-year-old bone handaxe from Konso, Ethiopia, shows advanced tool technology in the early Acheulean. Proc. Natl. Acad. Sci. Unit. States Am. 117, 18393–18400.
Sharon, G., 2007. *Acheulian Large Flake Industries: Technology, Chronology, and Significance*. Archaeopress. BAR International Series), Oxford.
Sherwood, R.J., Ward, S.C., Hill, A., 2002. The taxonomic status of the Chemeron temporal (KNM-BC 1). J. Hum. Evol. 42, 153–184.
Stanistreet, I., McHenry, L.J., Stollhofen, H., de la Torre, I., 2018. Bed II sequence stratigraphic context of EF-HR and HWK EE archaeological sites, and the Oldowan/Acheulean succession at Olduvai Gorge, Tanzania. J. Hum. Evol. 120, 19–31. https://doi.org/10.1016/j.jhevol.2018.01.005.
Stanistreet, I.G., Stollhofen, H., Deino, A.L., McHenry, L.J., Toth, N.P., Schick, K.A., Njau, J.K., 2020. New Olduvai Basin stratigraphy and stratigraphic concepts revealed by OGCP cores into the Palaeolake Olduvai depocentre, Tanzania. Palaeogeogr. Palaeoclimatol. Palaeoecol. 554, 109751.
Stoenner, R.W., Oa, S., Katcoff, S., 1965. Half-lives of argon-37 argon-39 and argon-42. Science 148 (3675), 1325.
Texier, P.-J., 2018. Technological assets for the emergence of the Acheulean? Reflections on the Kokiselei 4 lithic assemblage and its place in the archaeological context of West Turkana, Kenya. In: Gallotti, R., Mussi, M. (Eds.), The Emergence of the Acheulean in East Africa and beyond: Contributions in Honor of Jean Chavaillon. Springer International Publishing, pp. 33–52.
Toth, N., Schick, K., 2018. An overview of the cognitive implications of the Oldowan Industrial Complex. Azania 53, 3–39.
Trauth, M.H., Maslin, M.A., Deino, A., 2005. Late Cenozoic moisture history of East Africa. Science 309, 2051–2053.
Tryon, C.A., 2006. "Early" Middle Stone Age lithic technology of the Kapthurin Formation (Kenya). Curr. Anthropol. 47, 367–375.
Tryon, C.A., McBrearty, S., 2002. Tephrostratigraphy and theAacheulian to Middle Stone Age transition in the Kapthurin Formation, Kenya. J. Hum. Evol. 42, 211–235.
Tryon, C.A., McBrearty, S., 2006. Tephrostratigraphy of the bedded tuff member (Kapthurin Formation, Kenya) and the nature of archaeological change in the later middle Pleistocene. Quat. Res. 65, 492–507.
Uribelarrea, D., Martín-Perea, D., Díez-Martín, F., Policarpo Sánchez-Yustos, P., Domínguez-Rodrigo, M., Enrique Baquedano, E., Mabulla, A., 2017. A reconstruction of the paleolandscape during the earliest Acheulian of FLK west: the co-existence of Oldowan and Acheulian industries during lowermost Bed II (Olduvai Gorge, Tanzania). Palaeogeogr. Palaeoclimatol. Palaeoecol. 488, 50–58.
Wendorf, F., Schild, R., 1974. A Middle Stone Age sequence from the Central Rift Valley, Ethiopia. Institute for History and Material Culture, Polish National Academy, Warsaw.
Wilkins, J., Schoville, B.J., Brown, K.S., Chazan, M., 2012. Evidence for early hafted hunting technology. Science 338, 942–946.